

**Non-Contact Method to Assess the Surface Roughness of Metal Castings by 3D Laser**

**Scanning**

by

**Jaipravin Vijayarangan**

A thesis for Master submitted to the graduate faculty  
in partial fulfillment of the requirements for the degree of

MASTER OF SCIENCE

Major: Industrial and Manufacturing Systems Engineering

Program of Study Committee:

Frank Peters, Major Professor

Matt Frank

Vinay Dayal

The student author and the program of study committee are solely responsible for the content of this dissertation. The Graduate College will ensure this dissertation is globally accessible and will not permit alterations after a degree is conferred.

Iowa State University

Ames, Iowa

2017

Copyright © Jaipravin Vijayarangan, 2017. All rights reserved.

**DEDICATION**

I dedicate this thesis to my beloved parents, Mr. Subramaniam Vijayarangan and Mrs. Manjula Vijayarangan for making me who I am today. You have been with me every step of my life, through good and bad times and I'm thankful to you for sending me to the US and letting me pursue my passion. Thank you for believing in me, your guidance, support and unconditional love which have been instrumental in my success; and for instilling in me the confidence to achieve anything that I put my mind to. Thank you for everything.

## **BIOGRAPHY**

Jaipravin Vijayarangan was born to Mr. Subramaniam Vijayarangan and Mrs. Manjula Vijayarangan on September 26, 1989 in Ukkunagram (India), the spacious township of Visakhapatnam Steel plant which is an enviously green self-contained city often described as 'Green Paradise'. He received his Bachelor's degree in Mechanical Engineering from PSG College of Technology, Coimbatore in June 2011. He then joined L&T Valves as a Quality Engineer and excelled in his career track. Having felt the necessity to advance the inspection processes and delve deeper into the manufacturing techniques, he decided to pursue a graduate degree. In January 2015, he enrolled for his Master's program in the Industrial and Manufacturing Systems Engineering at Iowa State University. He started working as a Graduate Teaching Assistant for manufacturing labs from January 2015 and performed his research at the Rapid Manufacturing and Prototyping Laboratory (RMPL).

## ACKNOWLEDGMENTS

This thesis has become a reality with the kind support and help of many individuals. First, I would like to thank my major professor, Dr. Frank E. Peters for being a welcoming and friendly professor, for giving me the opportunity to work under him, for imparting his knowledge and expertise and for all the encouragement and support rendered during my two years at Iowa State. I would also like to express my special gratitude to Dr. Matthew C. Frank for always being helpful besides his busy schedule and for helping me understand the fundamentals of 3D scanning and for his valuable insights and suggestions. I would also like to thank Dr. Vinay Dayal for agreeing to be on the committee and providing me with useful inputs and resources.

I would like to thank my dear friend and colleague, Hieu Pham for helping me learn the approach one should have towards research and offering his timely help and support. I would like to thank Kevin Brownfield for his help in quickly making a test fixture and cutting test samples and Aaron Jordan for providing me with all lab essentials. I thank Ron Harns for training me on calibrating the FaroArm LLP. I would also like to thank Taylor Schweizer for his guidance in using the metrology equipment in lab and Wyman Martinek for providing contacts related to metrology equipment. I would like to thank Mike Hoefler for proactively answering my queries and research support group Kyle McNulty, Srikanth Ramesh, Zaine Talley, Niechen Chen for rendering their support when it was required. Special thanks to my friends Aparna, Arun, Dean, Goutham, Karthik, Nikhil, Nazareen, Suresh and Varsha for making my time at Iowa State University a wonderful experience. I remain indebted to my parents for always believing in me and supporting my decisions.

## TABLE OF CONTENTS

	Page
DEDICATION .....	ii
BIOGRAPHY .....	iii
ACKNOWLEDGMENTS .....	iv
ABSTRACT .....	vi
CHAPTER 1 INTRODUCTION .....	1
CHAPTER 2 LITERATURE REVIEW .....	9
CHAPTER 3 METHODOLOGY AND ANALYSIS OF RESULTS.....	14
Principal Component Analysis (PCA) .....	15
Equipment Used.....	19
Calibration settings used for Point Cloud Generation .....	21
Factors affecting point cloud generation during 3D laser scanning .....	26
Summary .....	35
CHAPTER 4 MODEL DEVELOPMENT AND IMPLEMENTATION FOR CHARACTERIZING SURFACE ROUGHNESS.....	36
Model Validation .....	38
Prediction of roughness on unknown quality surfaces .....	41
Experimental Castings .....	44
Validating the Scanning Method Using A Portable 3D Scanner.....	55
Zygo results on A1, A2, A3 and A4 .....	58
Test on 3D printed metal casting surface.....	58
CHAPTER 5 CONCLUSIONS AND FUTURE WORK.....	60
BIBLIOGRAPHY .....	62

**ABSTRACT**

This paper defines a methodology to estimate the surface roughness of metal castings by 3D laser scanning. The proposed method applies Principal Component Analysis (PCA) which transforms the point cloud of the casting surface into an orthogonal coordinate system. Using this coordinate system, the Root Mean Square (RMS) deviation of the surface peaks and valleys is estimated. This method is used to analyze the factors affecting point cloud generation and evaluate the technique used to obtain a consistent roughness parameter. A correlation curve was then established by plotting the roughness parameters obtained by PCA method against the corresponding root-mean square (RMS) readings on the cast micro finish comparator. Surface roughness measurements is performed on SCRATA 'A' plates and independent casting surfaces; whose roughness is previously unknown; is measured and the results are found to be consistent with the roughness values of the known cast micro finish comparator. The results from the surface comparators and areas of the scanned castings are also validated using a laser interferometer. The proposed method provides a fast, accurate and automated way of calculating surface roughness from the point cloud data. Its repeatability and versatility compares favorably with existing methods and would aid process control and standard interpretation.

## CHAPTER 1

### INTRODUCTION

Casting is a process in which molten metal flows by gravity or some other force into a mold made of sand, metal or ceramic where it solidifies in the shape of the mold cavity to form a geometrically complex part. The term casting can also be applied to the solidified piece of metal that is taken out of the mold [15]. All major metals and its alloys can be cast. The most common are iron, aluminum, magnesium, zinc, steel and copper-based alloys. Castings can range in weight from a few grams to several tons and this is showcased in Figure 1. As per facts published by AFS, 90% of all manufactured goods contain metal castings from 1956 metal casting facilities in the U.S. [1]

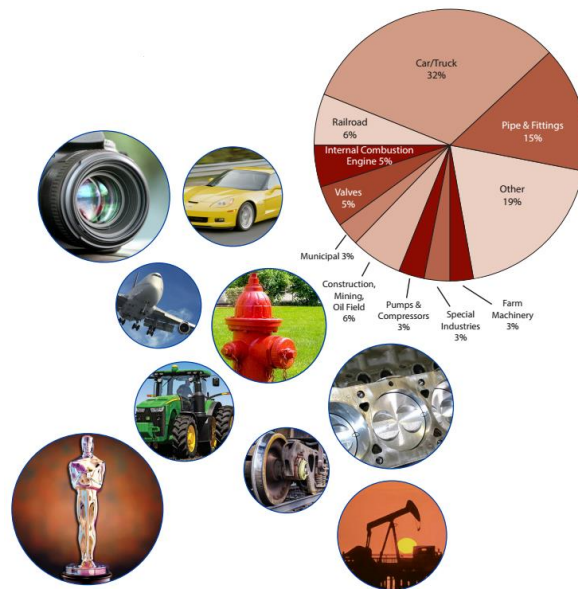
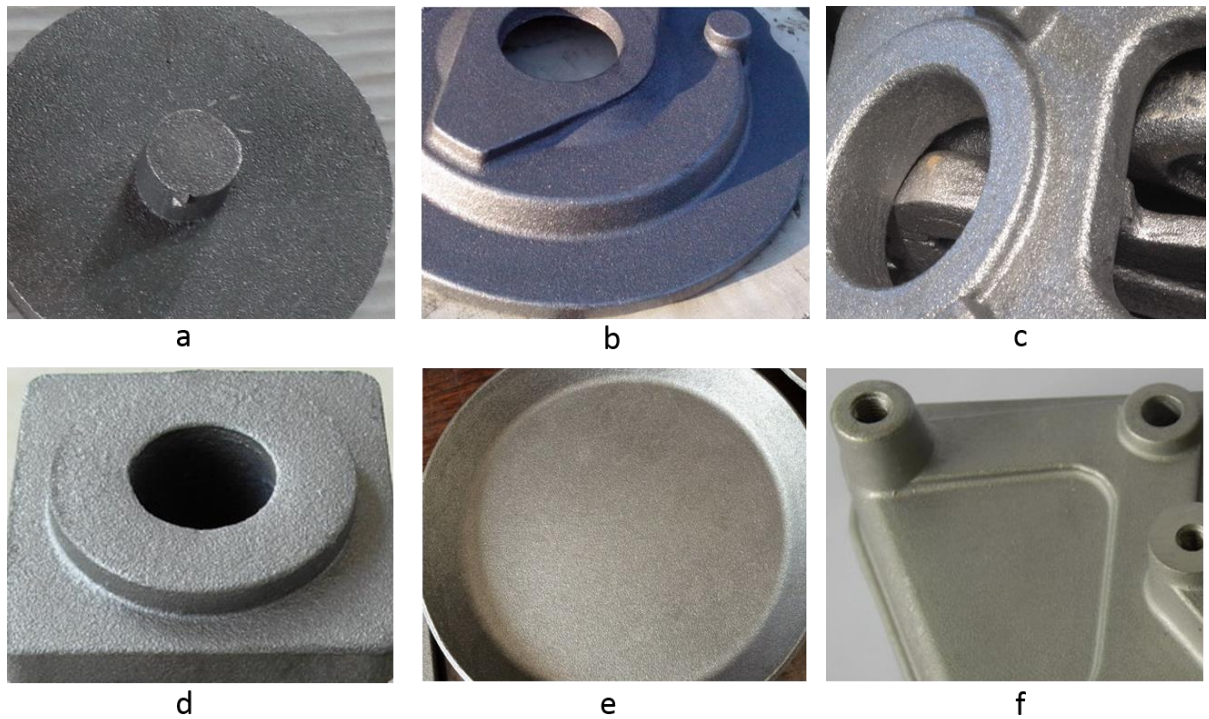


Figure 1: Pie chart showing the application of castings around the world with car/truck being the major user.

There are many types of casting processes. Some of them are green sand molding, no-bake sand molding, resin shell sand molding, permanent mold, die casting, investment casting (lost wax), lost foam, plaster casting and centrifugal molding. They are classified based on the composition of the mold material, or the manner in which the mold is made, or in the way the pattern is made. As castings are usually net-shape or near-net shape, surface finish becomes one of the key factors during process selection and varies greatly depending on the process being used as shown in Figure 2



*Figure 2: Typical surface finish quality of various casting processes a) Manual green sand (cast iron) b) Automatic molding, green sand (cast iron) c) No-bake sand (cast iron) d) Investment casting (Steel) e) Shell molding (cast iron) and f) Die casting (zinc)*

It can be observed from Figure 2 that smoothness levels vary based on the choice of casting processes and needs a standardized method to be characterized. This is due to diverse factors affecting the surface roughness, during the casting and processing stages of the manufacturing process. As per the BS EN 1370(2012), the surface condition of casting is influenced by the manufacturing process (expendable mold process, permanent mold process, etc.). Also, as weight and section thickness increase, the quality of surface finish decreases. It is noteworthy to mention that alloys with higher melting point produce lower RMS values than alloys with lower melting point. This can be attributed to the varying hot-strength of molds and cores based on the additives used. The higher the temperature, the more likely the degradation of the mold/core surface due to the radiant heat. In general, iron castings will not be as smooth as aluminum castings, and steel castings will be rougher. For permanent mold, coatings and routine mold die maintenance play a critical role whereas for sandcasting, a medley of factors come into play such as sand type, fineness of sand, additives used, type of compaction method etc. [2]. It is to be noted that for sand casting processes, sand makes up 80-90% of the molding material and cast finish is dependent on the quality of sand and preparation. Hence, a variation in any of these parameters could lead to bad surface quality.

Though there is no published standard for surface finishes obtained from various metal casting processes, according to the data gathered by Product Development and Analysis LLC (PDA), a table of values has been formulated using random samples from metal casting facilities in the US and abroad [2]. The capabilities from the participating metal casting facilities were used to create an average range as summarized in Table 1. The extreme low values are based on the lowest RMS values published in the literature.

*Table 1: Surface Finish Capabilities by Process (in RMS expressed in  $\mu\text{in}$ , with extreme low values in parentheses) based on [2]*

<b>Broad category of Casting Process</b>	<b>Sub-categories, RMS value range (extreme low value of RMS in <math>\mu\text{in}</math>.)</b>
<b>Sand Processes</b>	Shell, 75-150 (40) No Bake, 150-600 (40) Lost Foam, 125-175 (100) Horizontal Green Sand, 250-900 (100) Vertical Green Sand, 250-900 (100)
<b>Metal Mold Processes</b>	Die Casting, 90-200 (20) Centrifugal, 450-500 (100) Permanent Mold, 25-420 (180)
<b>Ceramic Mold Processes</b>	Plaster, 40-125 (25) Ceramic, 60-175 (25) Investment, 50-125 (32)

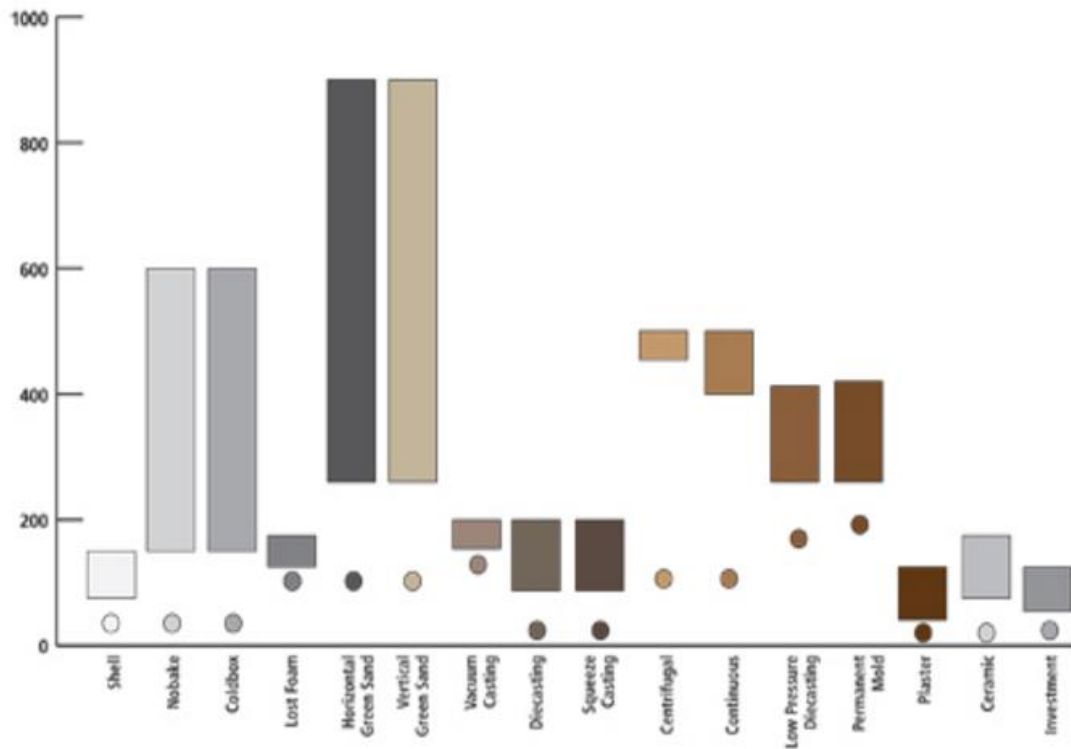


Figure 3: Bars represent the ranges of RMS values ( $\mu\text{in}$ ) each process is capable of producing. (Extreme low values are indicated by circles below the range) from [2]

From Table 1, it can be observed that casting processes can result in various surface finishes. It can be deduced that the most common process, sand casting typically produces an average root mean square (RMS) value of 250-900 micro inches. It can also be inferred from the lowest values given in parenthesis that sand processes generally produce the roughest surfaces. However, chemically bonded sand, including shell and no bake can compete with the ceramic processes when used at the most optimum setup with shell being in the most favorable range of average RMS values at 75-150 micro inches. It was also found that investment castings are effective at delivering the high gloss shine [2]. Figure 3 above shows an extensive graph depicting the roughness range typically obtained from various casting processes.

Specifications for the finished product often include requirements for tolerable surface finishes [20]. There has been no definite basis for measuring the surface finish of castings and has led to the emergence of surface inspection comparators such as ASTM A802, GAR micro finish Comparator C9, and ACI Surface Indicator scale which are shown in Figure 4b,4c and 4d. These comparators are widely accepted by the industry and it is reported that the use of ‘C-9’ comparators is recommended by specialists of the aircraft industry [12]. Foundries claim that they are in a position to offer castings in the range of specified surface finishes made possible by comparing their finished product with a cast surface finish comparator [Curley].

The assessment involves placing these comparators alongside the workpiece and comparing them by drawing the tip of fingernail at right angles across each surface. The

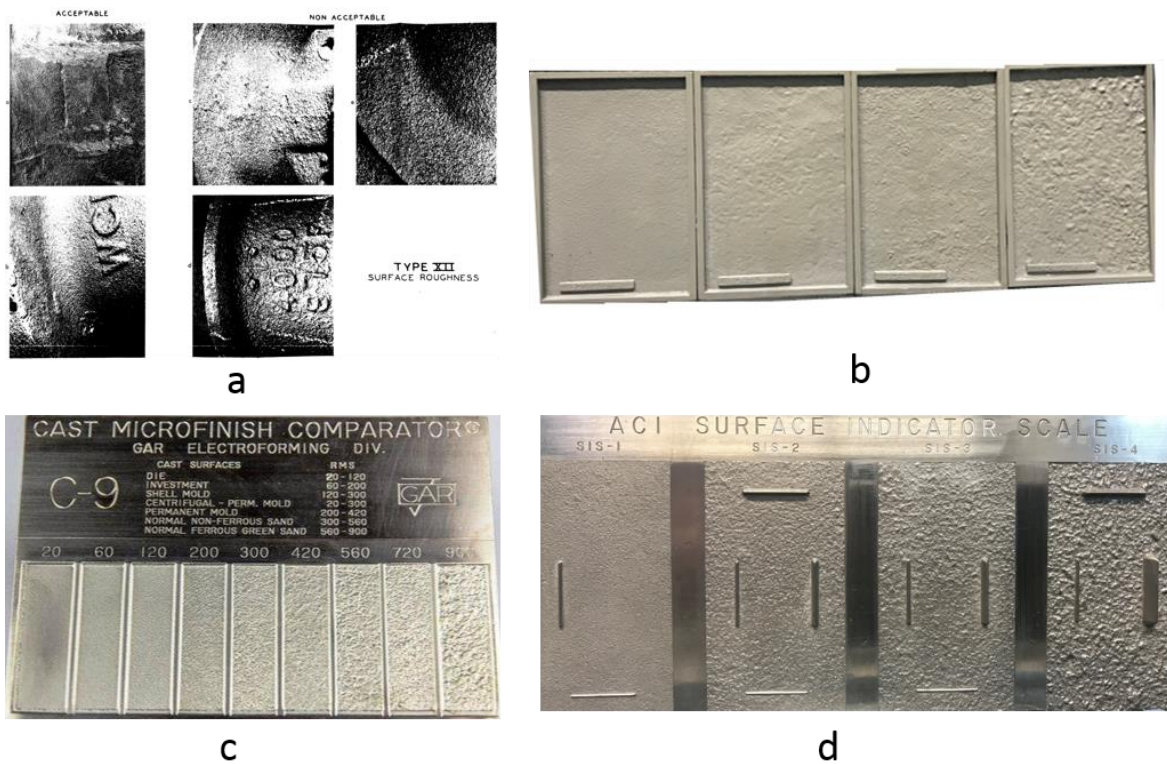
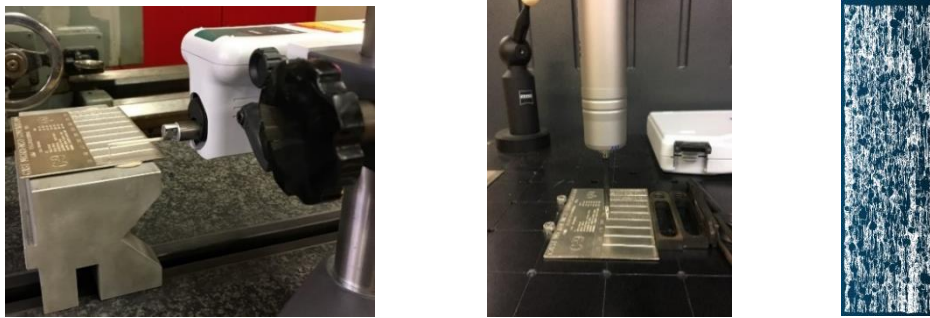


Figure 4: a) MSS-SP 55(Reference Photographs)[24] b) ASTM A802 Surface Texture plates c) Cast Micro finish Comparator (GAR) d) ACI Surface Indicator Scale

tactile feel of the fingernail contact must be the same if the finishes are identical. Figure 4a represents a visual comparison method called the MSS-SP-55 which has representative photographs for acceptable and non-acceptable surfaces. These assessments are highly subjective in nature and are highly dependent on the cognitive skills of the foundry inspector interpreting the comparator. Moreover, the end-user purchasing the product may not interpret the smoothness level as stated by the supplier and this leads to ambiguity at both ends. Further, these methods are qualitative in nature and this ends up in guesswork on the part of the manufacturer's inspector as to the actual requirements of the customer.

Contact methods such as a profilometer does not represent the entire casting surface and is highly variable between sample measurements due to Roughness Width Cut-off (RWC) and other limitations due to its measuring speed. Since the stylus probes of most instruments has a finite radius and the specimen's surface has abrupt or sharp angles at the bottom of the valleys, the profile measured by the motion of the stylus will be less than the peak to valley distance of the specimen. For example, rougher cast surfaces ranging from 420-900  $\mu\text{in}$  specimens on the cast micro finish comparators gave inconsistent roughness readings on the Mahr SD26 profilometer (Figure 5a) using a 0.01mm(394 $\mu\text{in}$ ) stylus due to surface peaks and valleys exceeding the range on the profilometer leading to considerable loss of motion. Although a Coordinate Measuring Machine (CMM) used in Figure 5b can serve as a better inspection system, the non-uniform texture of the casting surface, the available surface area of table relative to casting size and probe dimensions limits its usability for surface roughness estimations. That is to say, touch probe method using the CMM can obtain the accuracy needed but does not have the probe dimensions necessary to measure surface roughness. This makes them act as a low-pass filter not detecting high-

frequency valleys and would result in point cloud data as shown in the Fig. 5c. For example, a 0.5mm probe is relatively large compared to the peaks and valleys of the 720  $\mu\text{m}$  specimens and hence the probe would bounce along the top of the peaks and would not go into the valleys. Whereas, the CMM method of measuring surface roughness would work on machined surfaces since they have a definite, regular, repetitive and directional pattern. This is corroborated in the standard (BS EN 1370: 2012) that cast surfaces do not showcase the same cyclical character as machined surfaces and it is difficult to assess their roughness using conventional mechanical, optical, or pneumatic devices.



*Figure 5: a) Mahr SD 26 Profilometer, b) Zeiss CMM and c) 720  $\mu\text{m}$  point cloud generated by the CMM*

There is a need to provide a fast, versatile and accurate means for measuring surface roughness to aid process control and enhance standard interpretation thereby reducing unwarranted high cost due to scrap and repair and hence we proceed by way of 3D laser scanning.

## CHAPTER 2

### LITERATURE REVIEW

Visual inspection is by far the most commonly used technique for quality control processes.. Hatamleh et al. (2009) reported that the surface roughness is one of the most important parameters describing the surface integrity of a component since a significant proportion of component failure starts at the surface due to either discontinuity or deterioration of the surface quality. In the casting industry, qualitative surface inspection standards such as MSS-SP-55, ASTM A802, ACI Surface Indicator scale, BNIF 359 and GAR micro finish Comparator C9 are being used. As a result, a decision made on surface finish requirements solely based on the cognitive ability of the inspector with respect to the existing comparator plate's leads to conjecture thereby causing unwarranted high cost due to scrap and repair. Smith (1993) showed that humans have a reported effectiveness of 80% in repetitive assessment of products by visual inspection. A study by Daricilar et al. (2005) showed that there is a significant amount of repeatability and reproducibility errors in the visual casting surface inspection process. It was found that the average repeatability measurements of casting surface inspection was 63.5% whereas the average reproducibility measurements for the same were 45%. Watts et al. (2010) indicated that much of the casting surface is missed during the inspection stage due to various factors that affect the visual inspector's performance. Recently, a great deal of emphasis has been placed on developing a mechanical and optical aid to transform the subjective nature of visual inspection into a more reliable and quantifiable level [Quinsat].

Konstantoulakis et al. (1998) showed that the cast component (component geometry, component size, section size, etc.), the equipment available, and the alloy cast (melt

temperature, alloy type, melt head pressure) have significant effect on the casting surface quality. One naturally wonders how the interactions among the several aspects would affect the surface quality.

Moreover, the inability of contact type metrology instruments such as stylus profilometry to reproduce the exact topography of casting surfaces adds to the difficulty. Ambedkar (2016) showed that a touch-probe having a diameter more than or equal to the peak spacing will fail to capture the valleys that might be present in the two peaks making the probing systems unsuitable for metrology of irregular surfaces as shown in Figure 6b.

Luke et al. (2000) stated that the major disadvantage of the stylus instruments is that

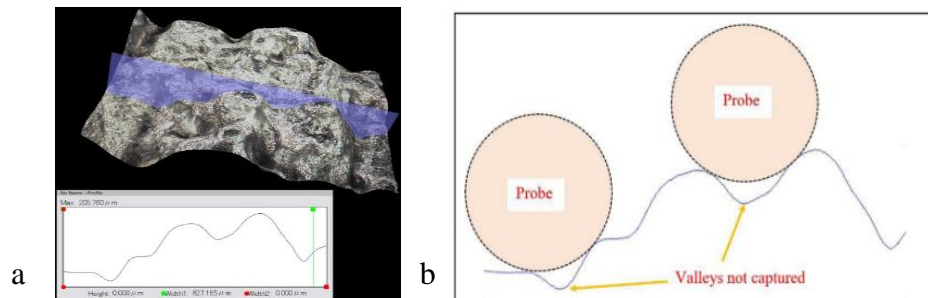


Figure 6: a) Microscopic (250x) image of an irregular AM surface b) A touch probe measuring an additively manufactured surface (Source [Ambedkar Graduate thesis, 2016])

they require direct contact which limits its measuring speed. In addition, since the instrument readings are based on limited number of line samplings, it does not represent the real characteristics of the surface. Nwaogu et al. (2013) also added that due to the randomly oriented deviations on casting surfaces, two-dimensional (2D) profile measurement may not describe the surface roughness of castings accurately. He also observed that contact-type instruments are difficult to work with on sand cast surfaces because of high surface roughness and material pick-up depending on the hardness of the surface being measured. Similarly, non-contact measurements using optical profilometry are not viable since

measurements are limited to small parts with constraint in orientation. Also, the small surface area the sample could cover and time taken adds to the difficulty. Luke et al (2000) mentioned that machine-vision systems are increasingly being used in industrial applications

Table 2: 3D data acquisition systems used in industry (from Ambedkar, 2016)

<b>Manufacturer</b>	<b>Type</b>	<b>Accuracy</b>	<b>Website</b>
Perceptron	Portable 3D scanner	-NA-	<a href="http://www.perceptron.com">http://www.perceptron.com</a>
Kreon	Zephyr II Blue Laser Scanner	10 $\mu$ m	<a href="http://www.kreon3d.com/3d-scanners/zephyr-2-blue">http://www.kreon3d.com/3d-scanners/zephyr-2-blue</a>
Nextec	Hawk	2 $\mu$ m	<a href="http://www.nextec-wiz.com/hawk_specs.html">http://www.nextec-wiz.com/hawk_specs.html</a>
FARO	ScanArm Edge	25 $\mu$ m	<a href="http://www.faro.com/en-us/home">http://www.faro.com/en-us/home</a>
Polhemus	FastScan	762 $\mu$ m	<a href="http://www.polhemus.com/scanning-digitizing/fastscan">http://www.polhemus.com/scanning-digitizing/fastscan</a>
GOM mbH	ATOS 3D scanner	-NA-	<a href="http://www.gom.com/metrology-systems/3d-scanner.html">http://www.gom.com/metrology-systems/3d-scanner.html</a>
Microscribe	Microscribe MX	50 $\mu$ m	<a href="http://www.3d-microscribe.com/MX%20Page.htm">http://www.3d-microscribe.com/MX%20Page.htm</a>
NextEngine	Desktop 3D Scanner	127 $\mu$ m	<a href="http://www.nextengine.com/products">http://www.nextengine.com/products</a>
Steinbichler	Comet5	-NA-	<a href="http://optotechnik.zeiss.com/en/products/3d-scanning/comet-l3d">http://optotechnik.zeiss.com/en/products/3d-scanning/comet-l3d</a>
Zoller+Fröhlich	Imager 5010X, 5010, 5006h	-NA-	<a href="http://www.zf-laser.com/Home.91.0.html?&amp;L=1">http://www.zf-laser.com/Home.91.0.html?&amp;L=1</a>
Konica Minolta	VIVID Series	50 $\mu$ m	<a href="http://www.3dscanco.com/products/3d-scanners/3d-laser-scanners/konica-minolta/">http://www.3dscanco.com/products/3d-scanners/3d-laser-scanners/konica-minolta/</a>

due to their ability to provide not only dimensional information but also information on product geometry, surface defects, surface finish and other product and process characteristics.

Swing (1963) stated that the single factor causing the most difficulty in devising a means of measuring surface roughness is that the surface characteristic has three dimensions. Therefore, it becomes necessary to average a multitude of readings for the third-dimension to

be included. With the advancement in vision-based 3D data acquisition systems that have extended machine-vision capability, a laser scanner that measures a large number of points on a three dimensional space with a reasonable accuracy could act as a powerful tool in surface quality inspection. Table 2 shows various 3D acquisition systems used in the industry with their reported accuracy [3].

Golnabi et al (2007) described that the measurement, gauging, integrity checking and quality control in a manufacturing industry have been advanced by the various 3D inspection techniques. Luke et al (2000) employed a micro-computer based vision system to derive the roughness parameters on tool-steel samples and proved that the proposed optical technique was better than traditional stylus technique in terms of repeatability and time efficiency. Whereas, Kocer et al (2015) conducted an experiment and showed that the surface roughness measurements obtained by 3D image processing method was similar to the values obtained by a profilometer on machined samples. It can be inferred that there has been limited research on estimating the surface roughness of castings by 3D scanning and the current methods such as stylus profilometry, optical microscopy and qualitative methods of visual inspection do not deliver repeatable results and are inefficient due to the time and cost involved. Hence, the motivation of this method to investigate 3D scanning.

## CHAPTER 3

### METHODOLOGY AND ANALYSIS OF RESULTS

This work proposes the method of 3D laser scanning and an automated way to calculate the surface roughness from point cloud data by a method known as Principal Component Analysis (PCA). This section also describes the recommendation of equipment, setting parameters, evaluation of technique and pre-processing information. This will also include the factors identified such as shininess, limits of scanning system, depth of field, scanning direction and point density.

In a three-dimensional coordinate system, the set of data points collected by the 3D scanner are defined by X, Y and Z coordinates. These data points, commonly known as *point clouds*, need to be trimmed so that extraneous points (edges, reflections, dust) can be avoided.

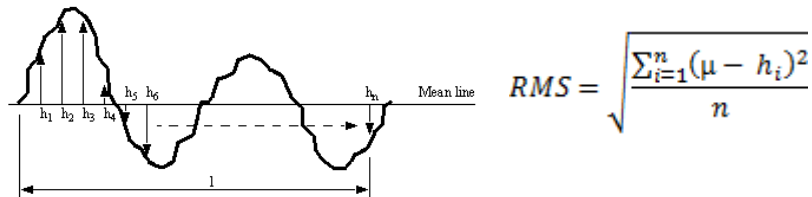


*Figure 7 : Typical 2D surface profile with computations of RMS*

*Surface roughness of cast surfaces is usually measured in terms of RMS (root mean square) value of variations from a nominal surface [Loftin]. A nominal surface ( $\mu$ ) can be defined as a surface that does not have surface irregularities and is geometrically perfect. Defined according to ISO 4287, RMS or  $R_q$  is defined as the root mean square value of the ordinate values  $z(x)$  within a sampling length and is depicted in Figure 7.*

However, it is practically recommended to measure roughness values over a number of consecutive sampling lengths to ensure that the  $R_q$  value is typical of the surface investigated [Leach]. Distinct from the 2D profile system that is highly variable between

measurements due to sampling length, it is proposed to calculate Sq, the areal extension of Rq, which is the root-mean square parameter of the surface departures,  $z(x,y)$  within the sampling area where A is the sampling area, xy.

$$Sq = \sqrt{\frac{1}{A} \iint_A z^2(x,y) dx dy}$$

However, since Sq is evaluated based on the assumption of a continuous surface as opposed to the discrete point cloud generated after 3D scanning, the parameter used in the proposed methodology is termed as a discrete version of Sq. Moreover, it is to be noted that surface texture measurements using coherent scanning interferometers or any surface texture measuring instruments calculate Sq over a discrete number of measuring points [20]. In this case, the equation would be written as follows with ‘N’ being number of scanned points and  $z_i$  is the z-co-ordinate of the  $i^{\text{th}}$  point:

$$Sq = \sqrt{\frac{1}{N} \sum_{i=1}^N z_i^2}$$

It is also to be noted that Sq has more statistical significance (it is the standard deviation) and is more sensitive to peaks and valleys than Sa [20]. Roughness calculations will be computed without the use of any filtering technique since determination of cut-off wavelength is not feasible without knowing the surface roughness beforehand. . Instead, a correlation curve will be established in relation to the standard roughness parameter that is discussed in detail under Chapter 4.

### **Principal Component Analysis (PCA)**

Here, a brief overview of principal component analysis used to estimate the nominal surface is given; for a detailed explanation refer to [Jolliffe]. Traditionally, PCA is a method to determine the number of uncorrelated variables in a large, high-dimensional dataset. These uncorrelated variables are called principal components which are axes that explain where variance is coming from. However, it is assumed here that this is known; namely, that the surface of the metal casting being measured explains most of the variation. Hence, in this research, the purpose of PCA is simply to try to find a representation of the nominal surface that can be used for further calculations.

Computationally, given a point cloud matrix  $X$ , the principal components are the eigenvectors of the  $\text{cov}(X)$ , that is, the covariance matrix of  $X$ . The most common way to find the eigenvectors is through a process known as the Singular Value Decomposition (SVD) [Golub]. If a point cloud  $X$  is first conditioned by centering each column, the SVD will give the principal components and the amount of variance attributed to each component [Wall]. After obtaining the principal components, the principal component scores are computed. Specifically, these are the new coordinates of the dataset in the space spanned by the

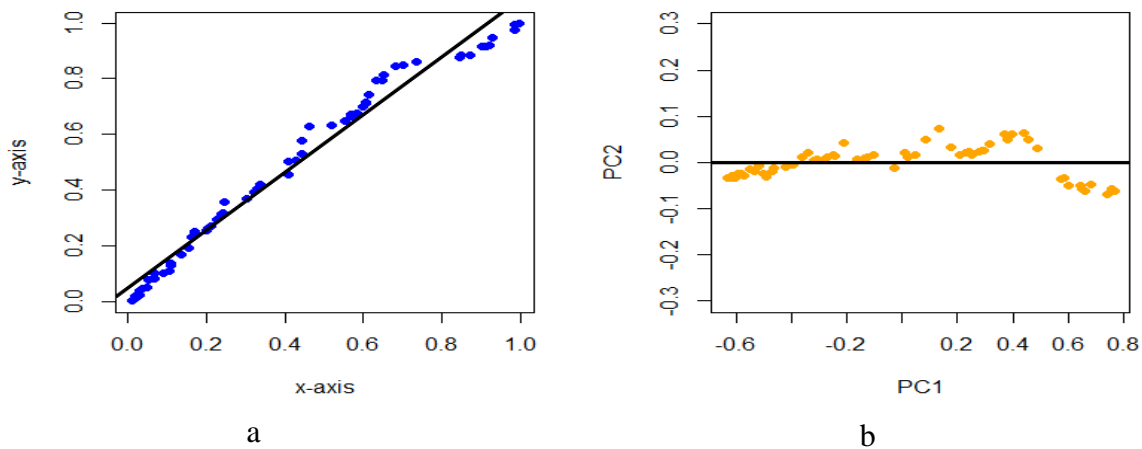


Figure 8: (a) Point cloud before PCA and (b) Point cloud after PCA

principal components. For better visualization, it can be observed from Figure 8a that the points are randomly oriented in the plane which is typically similar to the output from a scanning process. In Figure 8b, the points have been rotated so that orthogonal distances can be computed.

Ambedkar (2016) showed that PCA is an appropriate method for approximating surface roughness on additively manufactured parts after 3D scanning. Also, Tesfamariam (2007) demonstrated that PCA could be used to fit a plane to clustered point cloud data and results showed that laser scan data can be used to model and estimate rock surface roughness and had better results than traditional field observations.

With reference to measuring surface roughness, this transformation has been applied to obtain orthogonal distances from the best fit plane. For instance, in the first plot of Figure 9, if the regular least squares regression is applied, the residual will be minimized which is not necessarily an orthogonal distance. However, in the second plot in Figure 9, if the black line is treated as the nominal surface, the RMS can be computed as an estimate of the surface roughness. In other words, PCA is applied in order to approximate the nominal surface for any metal casting using an orthogonal distance to the surface.

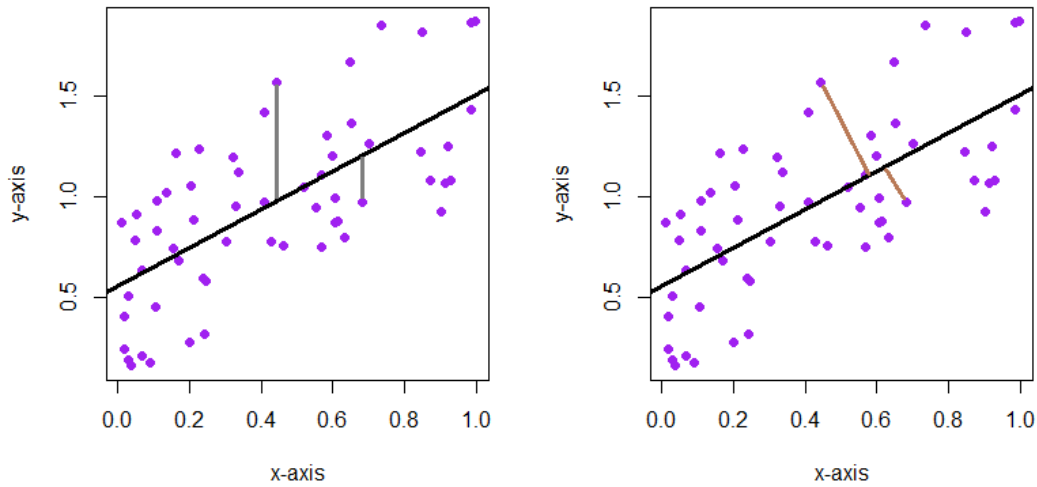


Figure 9: Comparison of distance estimation a) Least squares b) Orthogonal distances (PCA)

That is to say, an orthogonal regression plane is fit using PCA. In the developed R code, each coordinate,  $X$ ,  $Y$  and  $Z$ , is loaded from the point cloud into a data frame of size  $N$  by  $3$ , where  $N$  is the number of points in the scan. The PCA program is then applied to this data frame to fit a plane to the point cloud on the data matrix. In the end, this returns a  $3$  by  $3$  data frame containing the principal components; the first, second and third columns represent the ordering of the principal components, respectively. The first two columns, which are the first two principal components, span the 2-D space, that is, “X-Y plane”. The third principal component is orthogonal to the first two and defines the normal vector of the plane. Combined, this creates a new 3D coordinate system. To get the points in this new coordinate system, the centered  $N$  by  $3$  data frame is multiplied with the  $3$  by  $3$  matrix containing the principal components. In the end, an  $N$  by  $3$  data frame is obtained that contains the location of each point in the new coordinate system spanned by the principal components. Now, the residuals are simply the new  $z$ -coordinates since they are now referenced from  $X_0, Y_0, Z_0$ . In other words, by projecting the normal vector onto the X-Y plane, the peaks and valleys of the corresponding point cloud can be estimated. Typically, the distance could also be calculated

by subtracting the original data minus the fitted points and then calculating the signed distances from a point 'x<sub>0</sub>' to the plane containing 3 points given by the equation.

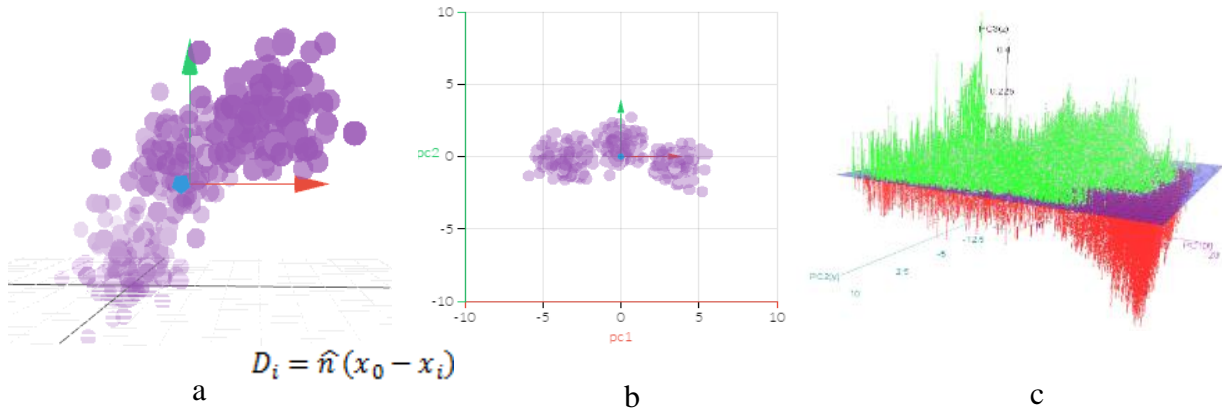


Figure 11: a) Scanned Point cloud, b) After performing PCA and c) Procedure showing determination of the fit plane of a scanned point cloud after peripheral trimming using PCA in R, points above the fit plane are colored green and the points below are colored in red

If a surface is measured using a profilometer or scanning interferometer, it is important that the surface being measured is not tilted related to the measuring device for optimal results and this is done using bubble level vials. Since PCA transforms the points into an orthogonal coordinate system by preserving the distance between points, this step would not be required. Moreover, returning the z-coordinates simply gives the height of each unique point. In order to visualize this process, Figure 10a & b shows a typical point cloud before and after applying PCA.

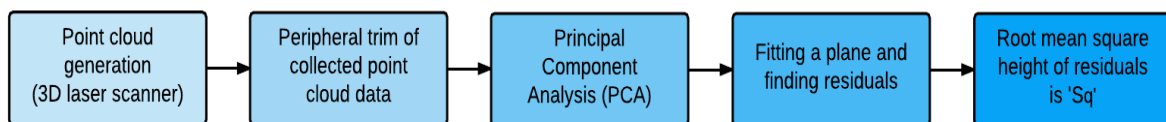


Figure 10: Methodology of surface roughness prediction based on Ambedkar (2016)

Figure 11 explains the general methodology of surface roughness characterization from point cloud generation to estimation of surface roughness. It is to be noted that Step 2 in Figure 11 namely the peripheral trim of point cloud data is optional and would not be required if the surface scanned is masked. Since the discrete  $S_q$  is calculated by the method of PCA plane fitting without applying smoothing filters, the roughness measured by this method is also termed as Primary profile roughness ( $P_q$ ) or PCA roughness values and has been used interchangeably within the document.

### **Equipment used**

There are various 3D data acquisition systems, namely active and passive. These systems differ in their working principle and use different mechanisms to interact with the surface of the part under observation. The 3D laser scanner used in this study is an active system that works on the principle of triangulation. It is a 7-axis, articulated arm with a spherical working volume. Every joint has a rotary optical encoder. The signals from these encoders are processed using advanced error coding and temperature processing technology [9]. Laser triangulation is accomplished by projecting a laser line onto an object and then capturing its reflection with a CCD (Charge-Coupled Device) located at a known distance



*Figure 12: Faroarm Edge with laser line probe.*

from the laser's source. This in turn reports the XYZ data of the scanned part based on the overall coordinate system of the arm, which is referenced by several encoders located in its articulations.

The laser line probe of 'Faro Arm Edge Version 1' shown in Figure 12 captures thousands of points using a red laser at a rate of 45,120 pts/sec is used to acquire the surface texture information from all the surfaces of standard comparators and the metal castings. The reported accuracy of the instrument is  $\pm 35\mu\text{m}$  giving a resolution of  $70.5\mu\text{m}$  at near field and repeatability of  $35\mu\text{m}$  [10].

### **Calibration settings used for Point Cloud Generation**

FARO CAM2 Measure 10 was used for acquiring point cloud data. Before performing the measurement session, a calibration procedure is performed on the hard probe and the Laser Line Probe (LLP) of the FaroArm Edge. This is done in the CAM2 Measure 10 software by resting the ball of the hard probe inside the calibration cone and taking points by pressing the green button on the probe and sweeping the probe across the various cuts of the cone. The last sweep is done in the vertical position by rotating the handle. Since, the results passed, the LLP was then chosen from the drop-down menu of the software and plane calibration was selected. The exposure settings was changed from automatic to fixed mode, then the hard probe was used to capture 9 points on the surface of the calibration plate. Having defined the plane with the ball probe and successfully passing the results, the screen prompted the user to calibrate the laser beam of the LLP on the same plane. By holding the line of the laser beam on the white surface, various laser line sweeps were recorded by sweeping the arm from left to right, front to back and finally moving it from near to far field

as part of the calibration sequence. Since the calibration test was successful, measurement session using FaroArm is continued.

Default values were used for all settings that include *material*, *scan rate*, *scan density*, *width threshold*, *noise threshold* and *peak threshold*. ‘Automatic-Normal’ was chosen for the exposure algorithm based on the recommended settings for compensation from the manufacturer. High-Accuracy Mode was enabled in order to improve the quality and 2Sigma value of the scanned data.

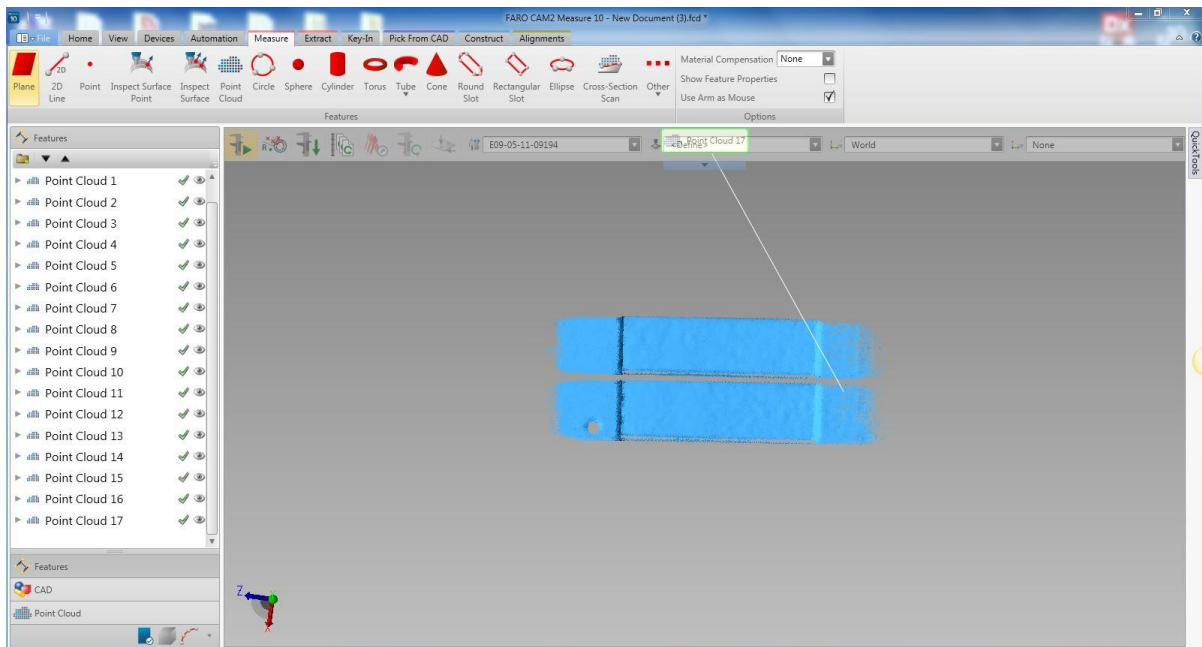


Figure 13 : Point cloud captured using FARO CAM2 Measure 10

A dense point cloud obtained after scanning a 300  $\mu$ m specimen is shown in Figure 13. In order to trim the unnecessary points along the areas of transition, an open source 3D point cloud processing software, CloudCompare, is used and the point cloud is edited and processed. This was required for the scanned point clouds generated on ‘C-9’, ‘ACI’ and ‘SCRATA’ comparator plates to eliminate the noise and to delineate the specimen boundaries before performing any roughness computations. Figure 14 shows the point cloud

loaded into the CloudCompare software; the original dataset is shown on the left, while the resultant one after trimming is showed on the right.

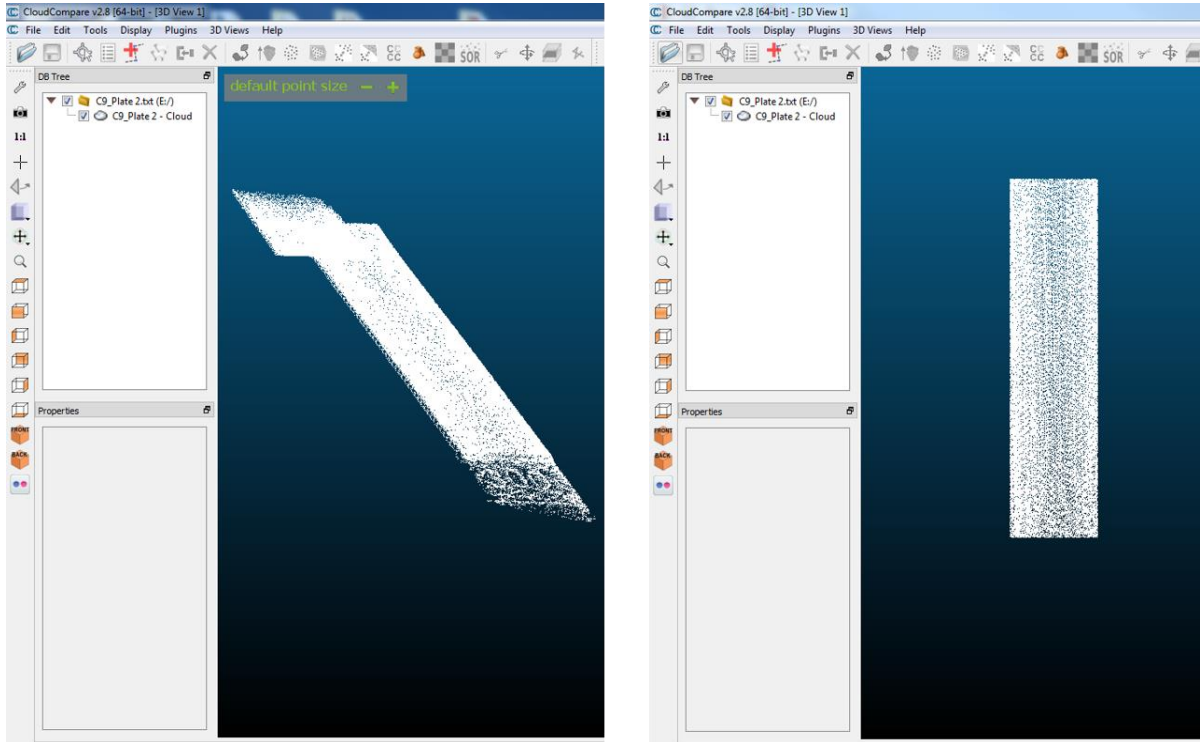


Figure 14: View of point cloud on the open source CloudCompare software before and after trimming

Since the GAR-‘C9’ micro finish comparator surface finish scale ranges from 20 to 900 RMS in micro inches (Figure 15), this comparator has been used to evaluate the effect of laser response and identify major sources of repeatability error in roughness calculations.



*Figure 15: ‘C-9’ Micro finish Comparator with varying surface finishes from 20 to 900 RMS*

The ‘C-9’ cast micro finish comparator is rectangular in shape and is a corrosion resistant electroformed duplicate of actual cast surfaces. These ‘C-9’ comparator plates are flat surface roughness specimens used for visual and tactile comparison. There are nine replicated cast surface finish specimens in this comparator and is particularly chosen since it covers a wide range of surface roughness specimens that a foundry can potentially cast. It is to be noted that this standard does not define any abnormality (protrusion or depression) as per ASME B46.1 [4].

To minimize the effect of luminosity on the scanning area, all laser scans are performed in a controlled environment free from any direct sunlight. From Figure 16, it can be observed that the surface texture of a casting is random and has no specific direction to it unlike a machined surface.

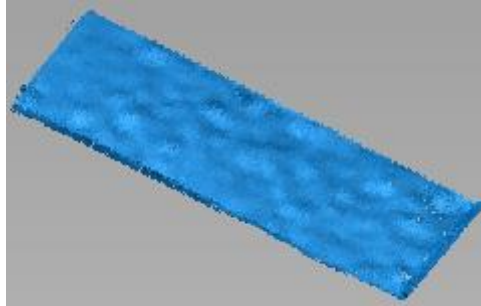


*Figure 16: Dense point cloud data generated by Faro on 900 RMS specimen of 'C-9'*

As shininess, surface texture, depth of field, scanning direction and point density play an important role in the system performance of a 3D laser scanner, a step by step procedure is adopted to determine the system sensitivity and identify the optimal set-up condition for predicting the surface roughness of metal casting surfaces. Each of these five factors chosen are explained and the results shown are explained in the following paragraphs. For the purpose of roughness estimations, all scans were performed at an illumination angle that was perpendicular to the object surface in order to maintain a constant beam spot diameter. The key factors calculated and analyzed values for surface roughness assessment are depicted below.

## Factors affecting point cloud generation during 3D laser scanning

### 1. Influence of dulling spray on smooth and higher roughness ranges:

It is known that reflectivity is detrimental to 3D data acquisition and hence it is a common practice to apply an anti-glare coating to objects before 3D scanning. Even though there are many 3D scan sprays in existence, for purposes of this experiment, a developer-based spray (Magnaflux SKD-S2) with a reported particle size of 2 microns was used to evaluate its effect on lower and higher ranges of roughness as shown in Figure 17. To start with, the 'C-9' Cast Micro finish surface comparator is used to evaluate this condition. Two roughness ranges, 0 200 and 900  $\mu$ in specimens were studied. To randomize the scans and to avoid any reflection from areas of transition, a high-performance black aluminum foil tape (T205-1.0) was used throughout the study to blackout the incident light on the edges and allow low light transmittance, thereby reducing noise. 11 scans each are made on 'C-9' with and without spray amounting to 22 *scans*. As stated earlier, all scans are performed orthogonally to the part's surface.



*Figure 17: Developer spray applied on patches 200 & 900 of 'C9' plate along with black masking tape*

A hypothesis test is carried out to check if there is any difference in means between 200 & 900  $\mu\text{in}$  specimens. This is done by applying the Welch Two Sample t-test using R. In each case, the assumptions are as follows:

$$H_0: \mu_1 = \mu_2$$

$$H_a: \mu_1 \neq \mu_2$$

Specifically, the null hypothesis is set so that the means are equal for ‘C-9’ with and without spray for ranges 200 & 900  $\mu\text{in}$  specimens. An ‘ $\alpha$ ’ level of .05 has been used for all statistical tests. In both the cases, the p-value is merely  $<.001$ . Since the p-value of the test is less than  $\alpha$ , the null-hypothesis is rejected. Hence, there is statistical evidence that dulling spray is required for ‘C-9’ and the same is applicable to the intermediate roughness ranges.

Next, to evaluate the effect of dulling spray on lower and higher quality levels of SCRATA A-plate [6], i.e. A1 and A4, scanning is performed 11 times each amounting to 22 *scans*. The same hypothesis test is carried out and for this case, the p-value is  $>.05$  for both quality levels. Hence, results show that there is no statistical difference in means with and without spray on these plastic replica casting surfaces.

Similarly, to evaluate the effect of dulling spray on metal casting surfaces, scanning is done for 11 times on surface of casting A (Figure 33) with and without spray each amounting to 22 *scans*. The same hypothesis test is carried out and in this case, the p-value is about  $<.001$ . Hence, there is statistical evidence that there is significant difference in means for the tested casting surface with and without spray.

In addition to the difference in means for metal casting surface, the standard deviation of estimated roughness values without applying developer spray was found to be *two* times higher than the standard deviation of the roughness values estimated after applying

developer spray. Even though the casting surface tested did not appear to be shiny in appearance, the results showed higher variance for roughness values without applying a dulling spray. Hence to improve the confidence in roughness measurements, the area of interest will be sprayed before laser scanning.

## **2. Influence of varying surface roughness:**

The next factor tested is to determine the effect of laser from the lower to higher surface roughness levels on 'C-9'. To randomize the scans and eliminate bias, two different 'C-9' comparator plates are scanned 11 times on each specimen amounting to *188 scans*. Since the 'C-9' comparators were shinier, as per the results concluded earlier, a developer spray was used to dull the specimens before scanning process.

After analyzing the results of the scans, there is a reasonable interaction in the roughness ranges of 20, 60 and 120  $\mu\text{in}$  specimens as the values plateaued during preliminary analysis. To further investigate the reasoning behind this pattern, a precision machined flat surface plate with a micro finish value of 10 RMS in  $\mu\text{in}$  (Figure 18) is scanned 11 times after applying the developer spray.



*Figure 18: Surface of a precision machined flat plate coated with dulling spray*

The results from the scan reveals that an average PCA roughness value of 1155  $\mu\text{in}$  was obtained from the scanning process and this value was similar to the values obtained on roughness ranges 20-120  $\mu\text{in}$  specimens.

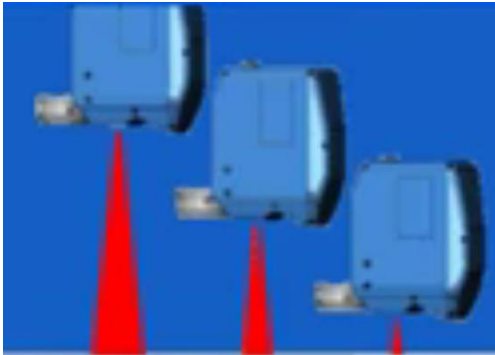
*Table 3: showing PCA roughness values obtained at 95% CI*

<b>Cast Specimen Name</b>	<b>Flat</b>	<b>20</b>	<b>60</b>	<b>120</b>	<b>200</b>
<b>PCA roughness value (lower estimate, higher estimate) in <math>\mu\text{in}</math>.</b>	(1145,1165)	(1066,1077)	(1053,1063)	(1055,1067)	(1307,1339)

It can also be seen from Table 3 that 20, 60 and 120  $\mu\text{in}$  specimens have no statistical difference due to confidence intervals overlapping. In other words, it can be understood that the scanning process gives erroneous measurement values on the lower range that is equivalent to the inaccuracy of the measuring system. These values could be the systematic variability of the non-contact scanning system since the scanner is unable to find a point better than its variability. For illustrative purposes, if a laser scanner would scan a granite surface that is flat, the scan results would reveal it to be a bumpy surface. Hence, 200 RMS which has a PCA roughness estimate higher than the flat plate is set as the minimum threshold for roughness calculations hereon. Also from Table 1 shown earlier, most sand casting processes have average RMS value starting from 250  $\mu\text{in}$  and hence these are suitable for the intended application. With the advancement of the non-contact technologies, there may be a different scanner and a different scanning setup that could estimate the roughness values on the lower range, but this is beyond the scope of this research.

### 3. Influence of depth of field:

Depth of field is an important performance factor in 3D laser scanning and is defined as the range over which the laser scanner can obtain an accurate image. Usually, scanners are equipped with a range finder to determine its distance from the scanned object and give feedback to the user often by LED functionality. It is known that by varying the stand-off distance, the resolution of the scanner changes. Also, it is to be noted that that all laser scanners are calibrated and tuned to be used in the calibrated ranges and resolution of scanner is up to the person scanning it. For example, if a scanner is at *near field*, it would yield high resolution. Figure 19 shows the variation in the depth of field along with tabulations of respective distances at corresponding depth of field [10].



Depth of Field	Distance
Far Field	3.54 inches
Standard Field	3.35 inches
Near Field	2.09 inches

Figure 19: Laser scanning setup showing Far, Standard and Near Field (left to right) along with respective distances at each depth of field for Faro Arm.

For visualization purposes, Figure 20 shows a feature measured with a scanner set at a large field-of-view. The image on the right shows a feature measured with a standard field-of-view which is at a relatively shorter standoff distance.

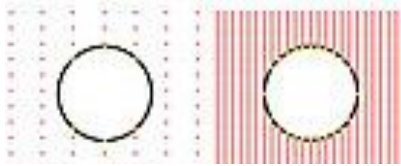


Figure 20: Example showing a feature with large and standard field-of-view

To determine the influence of depth of field on surface roughness measurements, three levels are studied namely near field, standard field, and far field after applying developer spray. 11 scans each are carried out on 200 and 900 specimens of two different ‘C-9’ comparators by varying the three factors amounting to 66 scans. Since the assumptions to carry out a one-way ANOVA is satisfied, this method is used for each specimen to identify if there is any difference in the means between the various fields. The levels chosen are near, standard and far for the factor illumination distance.

The null hypothesis is set so that the means of near, standard and far field are equal. Results obtained from the 200 and 900 specimens of ‘C-9’ comparator shows that the effect of depth of field is insignificant for lower roughness range but was significant for the higher roughness range, i.e.  $p=0.207$  for 200  $\mu\text{in}$  specimen and  $p<.05$  for 900  $\mu\text{in}$  specimen at an ‘ $\alpha$ ’ level of .05. In other words, the null hypothesis is failed to be rejected for 200  $\mu\text{in}$  specimen and null hypothesis is rejected for 900  $\mu\text{in}$  specimen. Based on the above statistical tests, it can be inferred that varying the depth of field causes a difference in mean RMS values at the higher roughness range, namely the 900  $\mu\text{in}$  specimen though there was no difference in mean RMS values on the lower roughness range namely the 200  $\mu\text{in}$  specimen. Analyzing

further, the coefficient of variation obtained for near, standard and far field on the 900 micro inch specimen did not show a significant difference and is summarized in Table 4.

*Table 4: Mean and Standard deviation obtained at varying depth of field for 900  $\mu$ in specimen*

	Near field	Standard field	Far field
Mean ( $\mu$ in)	4759	4826	4935
Standard deviation ( $\mu$ in)	117	100	109
Coefficient of variation (%)	2.46	2.07	2.21

Hence, it can be inferred that moving the scanner away from the standard field causes an increase in the coefficient of variation (CV). As a deduction for the FARO scanning system, all scans will be carried out at the standard field of view to reduce variance and increase the confidence in measurements.

#### 4. Influence of scanning direction:

To evaluate the effect of scanning direction on the lower and higher roughness specimens, two 'C-9' comparators were scanned in 3 different directions chosen arbitrarily at 0 degree, 45 and 90 degree (Figure 21) with constant depth of field. With this determined



*Figure 21: Laser scanning setup showing 0, 45 and 90 degree scanning direction along with a graphical schematic*

settings, roughness  $\mu\text{in}$  specimens namely 200, 300, 420, 560, 720 and 900 were scanned 33 times each amounting to 396 scans. It can be seen that the measured roughness values from 200  $\mu\text{in}$  specimen are increasing and the box plot data shows that the medians of 200, 300 and 420  $\mu\text{in}$  specimens are at the same level among respective scan directions at 0, 45 and 90 degrees. Since there is a slight variation observed in the box plot for 560, 720 and 900  $\mu\text{in}$  specimens, the relative error of the sample mean across each scanning direction is calculated with respect to its population mean and the results are displayed in Table 5.

*Table 5 : Relative error calculations for 560, 720 and 900  $\mu\text{in}$  specimens across varying scan directions*

Scanning direction	560-0	560-45	560-90	720-0	720-45	720-90	900-0	900-45	900-90
Relative error%	7.2	4.1	3.1	1.1	6.3	5.2	3.9	4.1	0.25

Hence from Table 5, it can be inferred that there is a minimal change in roughness values across scan directions. Therefore, it can be understood that there is no significant difference between the roughness values along different scanning directions on any roughness specimen from 200-900.

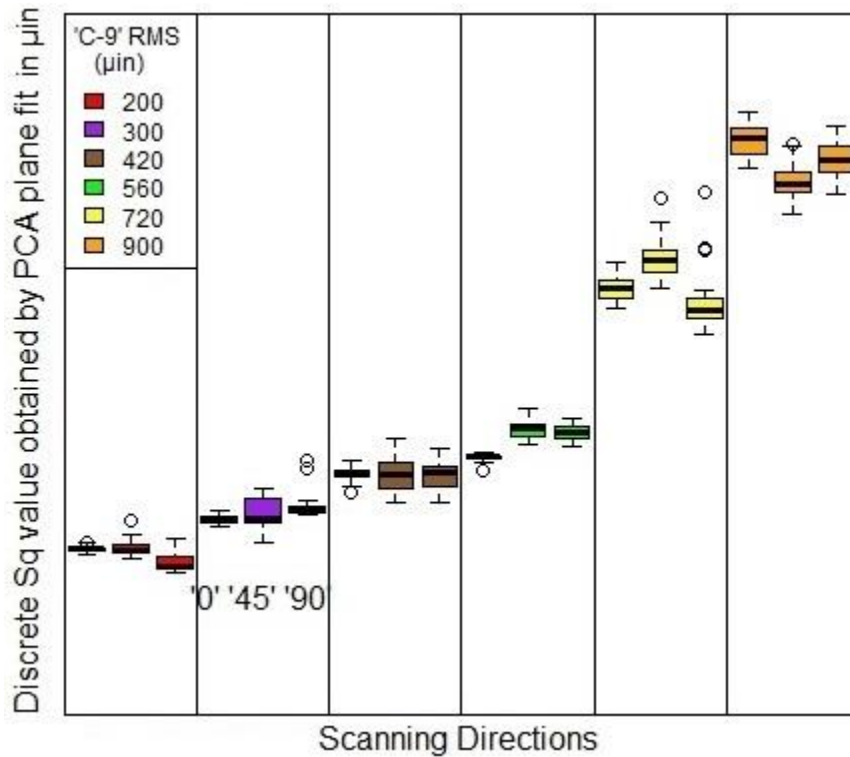


Figure 22: Box and Whisker plot showing the effect of scanning direction along the directions 0, 45 and 90 degrees for roughness specimens from 200-900 of 'C-9' comparator. The Box and Whiskers plot indicates the middle 50% of the data (box), the top and bottom quartiles of the data (outside the box), median (vertical line in the box), and outliers if present.

Hence, it can be stated that scanning direction does not influence the surface roughness measurements on casting surfaces and this can be attributed to the stochastic surface finish that is inherent on these surfaces unlike a machined surface that has a particular lay.

### 5. Influence of point density:

In laser scanning, the acquisition speed is equal to the scan rate which is the number of points captured per second. This is calculated by multiplying two values: frequency (number of laser lines recorded per second) and the number of points on each laser line. For example, a scanner with 752 points per line with a frames per second of 60 delivers a scan rate of 45,120 points per second. Since, each 'C-9' specimen covers a rectangular area approximating to 0.75 square inch units, the total number of points recorded over this defined

area can be termed as the point density. Depending on the depth of field and number of scan passes, one can achieve a higher or lower point density.

Keeping the factors such as standard depth of field, scanning direction and dulling spray constant, the point density over the defined 'C-9' area is systematically increased. To study the effect of point density in roughness calculations, the roughness micro inch specimens from 200-900 on the 'C-9' comparator are studied at 9 different increments starting from 5000 up to 100,000 points by varying the scanning speed and the number of times the laser line probe is swept across the same surface. It is to be noted that number of points chosen for comparison is approximated to the intended incremental points due to the inherent randomness in point generation.

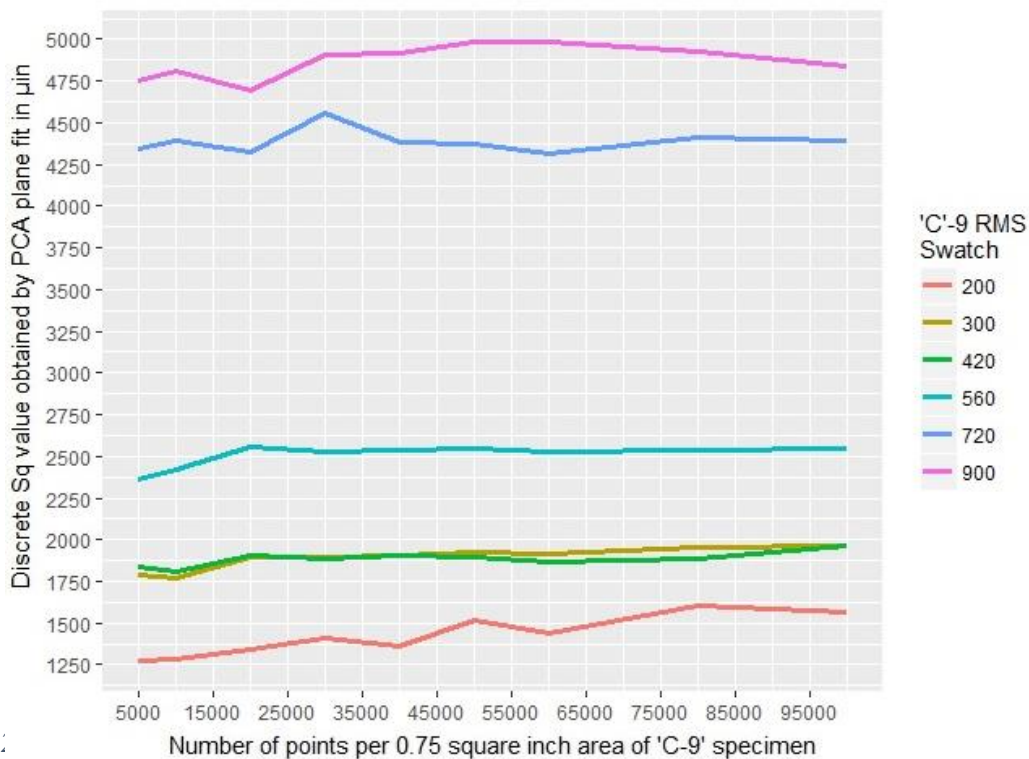


Figure :

es

The graph in Figure 23 shows that for varying point densities, the roughness value obtained are the same. Based on trials conducted at standard depth of field, it is recommended to achieve a minimum of 5000 points on the 0.75 square inch area of any 'C-9' specimen. It is to be noted that the 0.75 square inch area is only used for evaluation of the proposed technique on the available 'C-9' area and *should not be regarded* as a standard area for surface roughness measurement.

Based on all the factors studied, it can be summarized that a matte surface would be required for optimal laser response and that smoother roughness ranges from 20-120 micro inch specimens cannot be measured due to the systematic variability of the FARO scanning system. It was also found that scanning direction and point density does not influence the roughness calculations and this can be attributed to the stochastic surface finish of cast surfaces unlike machined surfaces. However, at varying depth of field, a difference in roughness values on the 900  $\mu\text{in}$  specimen of 'C-9' comparator was noticed compared to the 200  $\mu\text{in}$  specimen. However, there is an increase in the coefficient of variation of PCA roughness values when moved away from the standard field. Thus, to obtain a better sensitivity of the system and increase the confidence in measurements, standard field of view was selected for subsequent measurements on the FARO scanning system.

The results from the preliminary data collection were used to determine the optimum condition needed for laser scanning and this would be used as a baseline to conduct further experiments and build a correlation between obtained PCA values and standard roughness values stated on the comparator plate.

## CHAPTER 4

### MODEL DEVELOPMENT, VALIDATION AND IMPLEMENTATION FOR CHARACTERIZING SURFACE ROUGHNESS

This chapter focuses on developing a roughness estimation model where three identical comparator plates of ‘C-9’ are scanned 55 times each from 200-900  $\mu\text{in}$  roughness specimens amounting to 990 scans.



*Figure 24: Fixture used in study to bolt the three 'C-9' comparator plates*

In other words, this method is a calibration of the PCA estimated global surface roughness values of the 1.5”x 0.5” specimen in reference to the standard roughness parameter that has been estimated by the comparator industry [12]. It is to be noted that ‘PCA roughness values’ and ‘discrete Sq values calculated by PCA’ has been used interchangeably within this document. Due to the thin design of ‘C-9’ comparator plates, a custom-made fixture as shown in Figure 24 was built to secure the three comparator plates and ensure consistency between scans.

The PCA roughness values is different from the roughness values stated on the comparator since the proposed method does not remove longer wavelength shapes known as waviness. In other words, the primary surface roughness refers to the primary profile that includes roughness and waviness. In order to evaluate this phenomena, a profilometer was used on a 900 $\mu$ in specimen of 'C-9' comparator plate. In Table 6, the primary profile (Pq) and waviness (Wq) of this comparator plate have been compared to three random PCA roughness values.

*Table 6: Primary profile roughness (Pq) at 0.1 inch cut-off wavelength (Lc) on 900 $\mu$ in specimen of 'C-9' comparator plate. \* represents that the plate was sampled 10 times using the stylus profiler to generate three values and cannot be regarded as representative 'Pq' roughness value on the 900 $\mu$ in*

C-9 Cast Micro finish Comparator			
	'Pq' estimated by stylus profilometry on traced profile ( $\mu$ in)	'Wq' estimated by stylus profilometry on traced profile ( $\mu$ in)	PCA method on scanned point cloud ( $\mu$ in)
1	3675*	2976*	4646
2	3295*	2488*	4384
3	3105*	1992*	4850
<b>Average</b>	3358	2485	4626

It is to be noted that as per ISO 4288, the desired cut-off wavelength (Lc) for measuring a non-periodic profile of 900  $\mu$ in roughness is *0.3 inches*. Due to z-axis limitations on the Mahr SD 26 profilometer, 0.1 inches was used as the cut-off wavelength for trial purposes. It is also important to note that the 'Pq' and 'Wq' values shown in Table 6 were sampled multiple times to sample smoother points and generate a roughness value that was within the z-range of the profilometer. Hence the tabulated values should not be regarded as a representative value for the 900  $\mu$ in specimen and purely for illustrative purpose.

Since the surface finish refers to the "roughness" aspects of the surface ignoring the shape and underlying waviness, surface measurement is performed by 2 important steps

namely fitting and filtering prior to the output of roughness number. Traditionally, the first step involves “fitting” of a geometric reference such as a line or plane (2D or 3D) using least squares regression. We use PCA to fit a geometric reference plane as depicted in Figure 9 of Chapter 2. In other words this step ignores any form error. It is to be noted that PCA plane fitting can be performed only if there is no form error in the part being scanned. For example, this step cannot be performed if the surface is curved. Hence, the resulting roughness calculations after the first step is called Primary Profile Roughness, common ones being  $P_q$  (root-mean square deviation) and  $P_a$  (arithmetic average). The values shown under Table 1 correspond to the  $P_q$  values obtained using profilometer versus proposed PCA method. The second step would be to separate the waviness and the roughness of the selected points. In other words, running a smoothing filter through the primary data would accomplish this. The amount of smoothing is based on the filter cut-off wavelength. The cut-off wavelength is the wavelength that separates shorter wavelength from the longer wavelength. Shorter wavelengths fall into the roughness profile and longer wavelengths appear in the waviness profile. A “Gaussian” filter is recommended in ASME and ISO standards. Changing the filter cut-off value would change the amount of “averaging” and “smoothing” and can have a huge impact on the measurement of roughness and waviness. Choosing a smaller cutoff value will result in smaller roughness values even though the real surface could be very rough. For this purpose, a table of “standard” cutoff values along with selected recommendations is provided for non-periodic profiles in ASME B46.1 and ISO 4288. However, use of this table requires assessment of the surface texture by a single measurement that is representative of the surface which is not possible since the roughness is unknown beforehand. Hence for characterizing the surface roughness, the set of PCA roughness values obtained from the

extensive scan results of three independent ‘C-9’ comparator plates (990 scans) would be used. A correlation curve is plotted between the average PCA roughness values obtained on each specimen against its corresponding average roughness value stated on the comparator.

Looking at the trend of PCA roughness values of scanned comparator plates in Figure 25, it is likely that further extrapolation of the best-fit line would be similar to a log function as opposed to an exponential function and hence it is appropriate to use logarithmic regression in this case. The equation of this correlation curve will be used to predict the surface roughness of unknown cast surfaces. It is to be noted that the upper half of the best fit trend line is extrapolated beyond the range of the collected data.

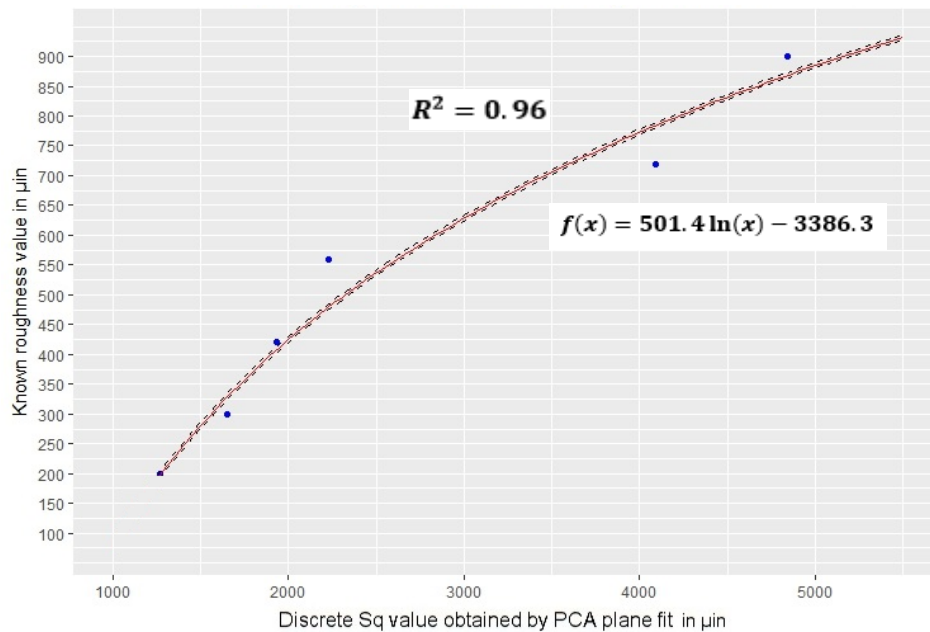
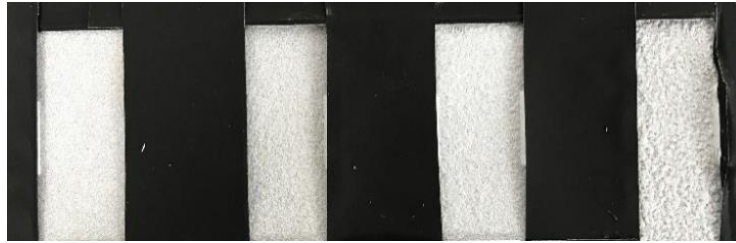


Figure 25: Plot showing known roughness values on comparator (after filtration) against the PCA roughness values. Graph also shows the calculation of the fitted values (red line), mean (blue dots) and 95% confidence interval (black dotted line) and the predicted equation

### Model Validation

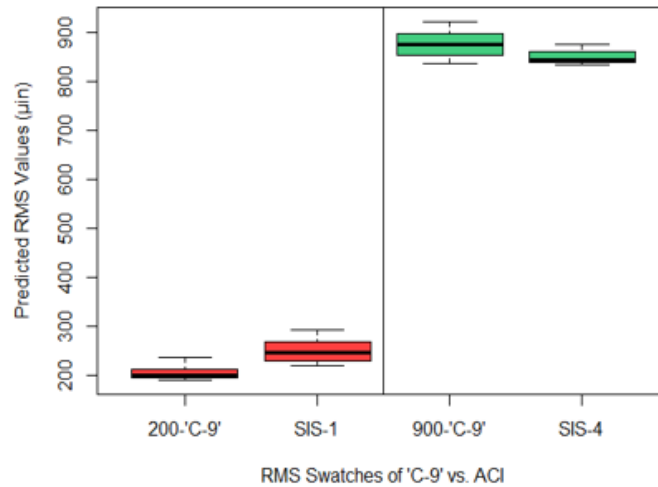
To validate the effectiveness of the model, an ACI Surface Indicator scale is used as depicted in Figure 26. This scale which is an exact replica of the surfaces of four high alloy castings is considered representative of modern production methods developed by the Alloy Casting Institute. These test castings were supplied by different foundries in several alloy compositions and were produced by ceramic, shell and conventional sand molding techniques [29]. Shown in Figure 26 are the four surfaces of the scale reproduced in nickel by electroforming process.



*Figure 26: ACI Surface Indicator scale showing 200, 350, 500 and 900 micro inch specimens with developer spray and black masking tape*

To start with, the common roughness specimens between ‘C-9’ and ‘ACI’ are chosen namely the SIS- Level I (200  $\mu\text{in}$ ) and SIS – Level IV (900  $\mu\text{in}$ ). These specimens of 1.5” x 0.5” are scanned 14 times each amounting to 56 *scans*.

The RMS values obtained from this model shows consistent measurements with relatively smaller variations as can be seen in Figure 27.



ACI Specimen Number	200	900
RMS Value (lower estimate, upper estimate)	(236, 264) $\mu\text{in.}$	(843, 859) $\mu\text{in.}$

Figure 27: Box & Whisker plot showing the RMS comparison between equivalent RMS specimens (ACI specimen number) of 'C-9' and 'ACI' and 95% confidence interval computed for 'ACI' specimens in the table below the plot. For plot description, refer Figure 22.

The variation in the estimated roughness values between these two specimens can be attributed to different surface textures on 'ACI' roughness specimens and also shows that the proposed method works on a completely different surface texture and validates the sensitivity of the developed method to the changes in surface features. In other words, it is clear that the spread and median of the roughness values on two similar specimens are close to each other and validate our characterization method.

To check the validity of developed model on roughness ranges that aren't originally on the 'C-9' comparator plate, the intermediate roughness specimens of ACI, namely SIS-2(350  $\mu\text{in.}$ ) and SIS-3(500  $\mu\text{in.}$ ) are used. These specimens are scanned 14 times each.

From Table 7, it is found that the obtained values on the intermediate roughness specimens are closer to the comparator values and this reinforces the soundness of the built correlation curve and characterization method.

Table 7: 95% confidence interval of  $\mu\text{in}$  specimens (cast specimen number) 350 and 500 on ACI plate.

ACI Specimen Number	350	500
RMS Value (lower estimate, upper estimate)	(380, 399) $\mu\text{in}$ .	(433, 448) $\mu\text{in}$ .

In order to estimate the accuracy of the proposed surface characterization, the ACI surface indicator was chosen and a plot of the same is shown in Figure 28.

The table appended below the plot in Figure 28 shows the experimental error values

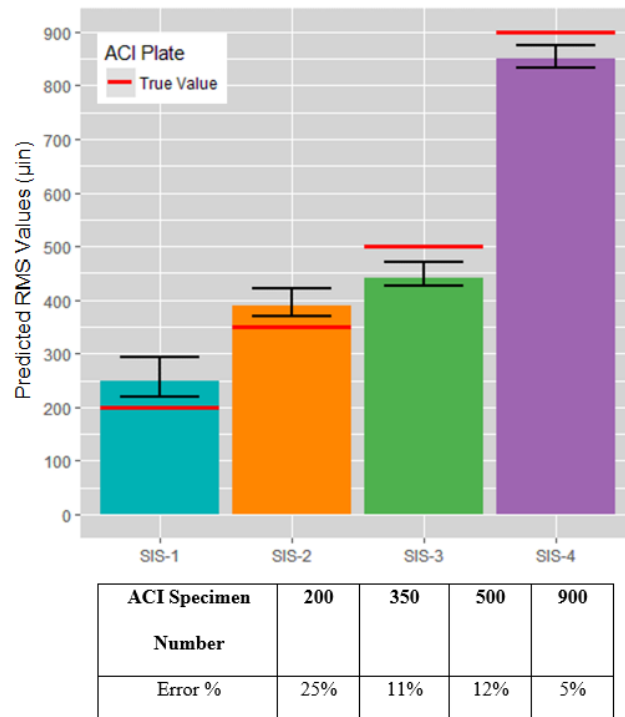


Figure 28 : Bar plot showing predicted average discrete  $S_q$  values of 4 different specimens of ACI comparator plate plotted as a function of its true value shown as a red solid line. Error bars represent minimum and maximum values (range) obtained at every specimen. The table below shows the % of experimental error.

between the measured roughness value and its accepted value. It can be inferred from the maximum percentage error, that the measurement system is at an acceptable level and the higher error percentage of 200  $\mu\text{in}$  roughness specimens can be attributed to the systematic variability of the scanning system on smooth surfaces as explained earlier.

### **Prediction of roughness on unknown quality surfaces**

Having predicted the roughness on known casting surfaces, the next step is to characterize the surface roughness of unknown casting surfaces. It is well-known that roughness is a localized phenomenon and in-order to better estimate the surface roughness of a casting surface over a specified area, certain guidelines need to be followed. It is to be noted that most precision reference standards that have a calibrating block recommend that at least 5 different traces are to be made over the specimen to determine the arithmetic average value on each patch [11].

With respect to casting surfaces, since the model is built on ‘C-9’ scans made over a rectangular dimension of 1.5”x 0.5”, we arbitrarily chose thrice the area of ‘C-9’ as a minimum area of scan and averaged the 3 segments to approximate the surface roughness values.



*Figure 29: ASTM A802 – SCRATA Surface Texture Plates (left to right- A1 to A4)*

In other words, the method proposed uses multiple smaller samples equivalent to the specimen dimensions of ‘C-9’ with the assumption that the underlying surface is smooth. Specifically, the actual geometry of chosen casting sample post shrinkage is smooth without roughness and abnormalities similar to the underlying surface of ‘C-9’ and ‘ACI’ specimens scanned earlier. Figure 30 shows one of the widely used SCRATA texture plates ‘A1-A4’ in which the lower left-area free of any curvature approximating to 1.5” x 1.5” dimensional area is chosen and scanned 14 times each on A1, A2, A3 and A4 amounting to 56 scans. 42 segments are analyzed for each SCRATA plate. The results obtained at 95% confidence interval have been tabulated in Table 8 and Figure 30.

*Table 8 : Corresponding SCRATA levels and computed PCA values, average RMS (discrete Sq) using co-relation curve. Numbers are in the form  $\mu$ in ( $\mu$ m).*

<b>SCRATA Texture Levels</b>	<b>A1</b>	<b>A2</b>	<b>A3</b>	<b>A4</b>
Average PCA values of the primary surface in $\mu$ in ( $\mu$ m)	2828 (72)	3762 (96)	5637 (143)	6302 (160)
Average RMS Values (Sq) using correlation curve in $\mu$ in ( $\mu$ m)	599 (15)	742 (19)	944 (24)	1003 (26)
Standard Deviation $\mu$ in ( $\mu$ m)	109.22 (2.7)	110.17 (2.8)	147.18 (3.7)	33.42 (0.8)

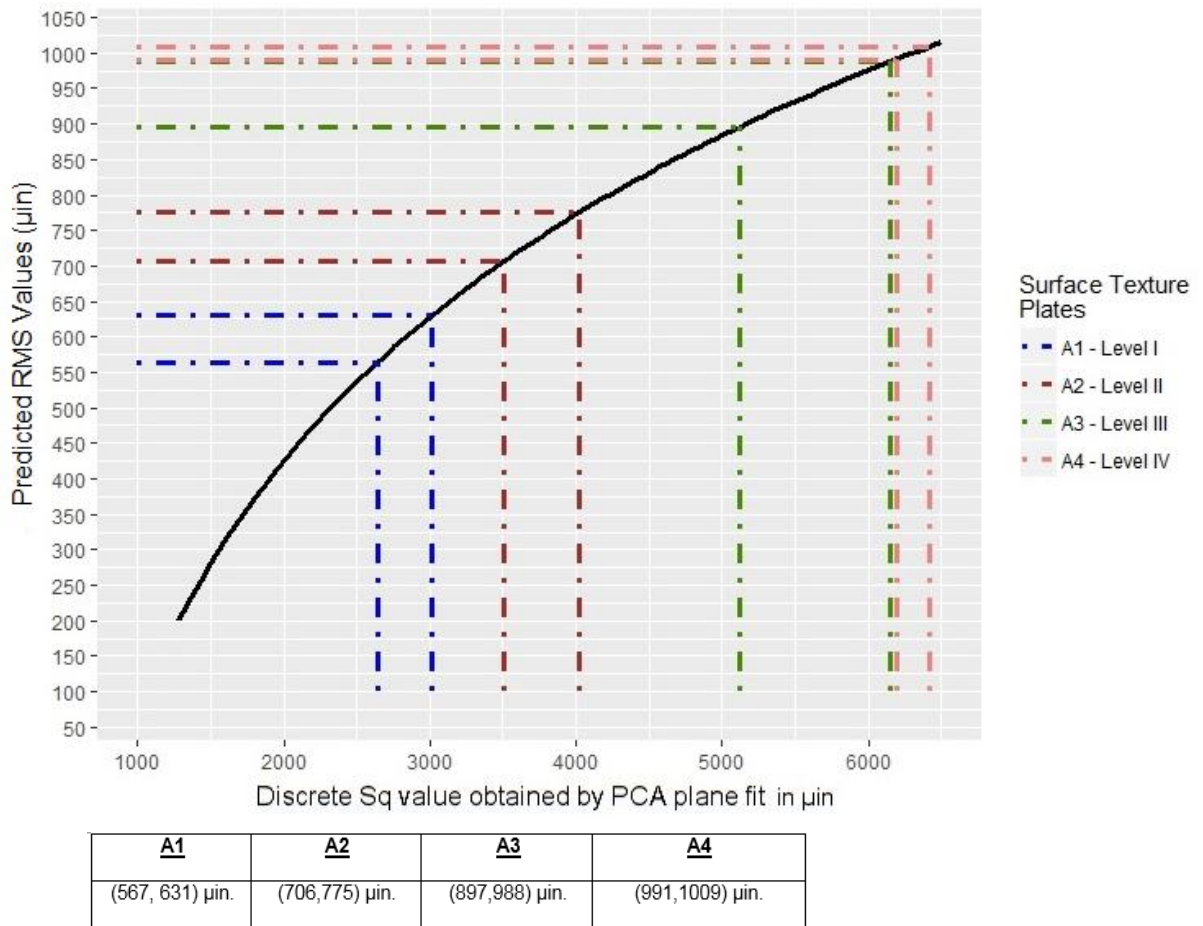


Figure 30: The dashed lines represent the 95% confidence interval of the ASTM A802 SCRATA plates. These indicate the level of uncertainty about each value on the graph. Longer/wider intervals mean more uncertainty. Black line represents the fitted model built in Figure 25. The confidence intervals are tabulated below the graph.

Nwaogu et al. (2013) identified similar trends in his surface roughness characterizations using microscopy that an ‘A1’ surface is approximately equivalent to  $16.47 \mu m$  and an ‘A2’ surface is approximately equivalent to  $20.47 \mu m$ . However, these scanning probe microscopes are not versatile and time-consuming for surface roughness measurements when compared to a laser scanner.

While it is reasonably certain that the four groups of SCRATA ‘A’ plates are truly different, the discontinuity existing between various quality levels showcase the current problem that we have at hand. Looking at this level of uncertainty as depicted in Figure 30, it

can also be understood that a subjective evaluation of a metal casting surface would lead to confusion between the manufacturer and the customer leading to misinterpretation of standard. This ambiguity would also lead to disagreement causing unnecessary repairs and delay in meeting delivery schedules. Hence, quantifying the surface roughness would be the solution to this industrial problem rather than using comparator plates.

To further validate if the proposed method classified independent SCRATA plates as per the predicted confidence intervals shown earlier in Figure 30, three miniature A-plates namely A1, A3 and A4 shown in Figure 31 are scanned 9 times each on 1.5”x1.5” area and segmented into three slices of 1.5”x0.5” amounting to 27 scans and 81 segments. The estimated averages of A1, A3 and A4 are shown in Table 9.

*Table 9: Estimated average RMS and standard deviation on miniature SCRATA plate.*

<b>SCRATA Texture Levels</b>	<b>A1</b>	<b>A3</b>	<b>A4</b>
<b>Average RMS Values</b>	559 $\mu\text{in}$	978 $\mu\text{in}$	1043 $\mu\text{in}$
<b>Standard Deviation</b>	27.81 $\mu\text{in}$	17.21 $\mu\text{in}$	10.31 $\mu\text{in}$



*Figure 31: Miniature A1, A3 and A4 plate used to test our model*

The average RMS value of ‘A1’ lies just outside the predicted confidence interval; regardless, it would still be classified as an ‘A1’ surface. It should also be noted that the RMS deviations of plate ‘A4’ was outside the predicted confidence interval.

The results of surface characterization using the proposed method of laser scanning is consistent on an independent SCRATA plate and hence an additional feature has been added to the developed program. Resistance to change is a common part of any organization and to aid the slow transition from qualitative standards of inspection to reliance on quantitative method, additional lines of code have been built into R, a statistical computing software, that would not only output the surface roughness of the casting in micro inches and microns, but also displays the equivalent approximated surface texture level as shown in Figure 32. It is to be noted that, the ends of the confidence intervals are extended to the beginning of the next interval.

```
> d=Roughness("A1_1 - cloud.txt")
[1] "The approximated RMS value(Sq) is 617 μin. ( 15.7 μm.)"
[1] "The approximated Sa value is 517 μin. ( 13.1 μm.)"
[1] "Note: For reference purpose only, the surface texture is'
      approximately equivalent to ASTM A802 A1-(Level I)"
```

*Figure 32: Output script readout from R- console after inputting the point-cloud from A1 comparator scan*

### **Experimental castings**

Laser scanning of metal casting surfaces is performed to estimate the roughness values and demonstrate the usefulness of proposed method on production castings. For this purpose, three different castings of varying design and section thickness are used.

To check the repeatability of the roughness measurement on identical casting surfaces, three similar castings are chosen under each category.

#### **1) Casting A :**

The first test is carried out on a casting A (Figure 33) with uniform section thickness on an area of 1.5”x1.5”, scanned 5 times each and segmented into equivalent ‘C-9’ size. The results obtained are plotted in Figure 33.

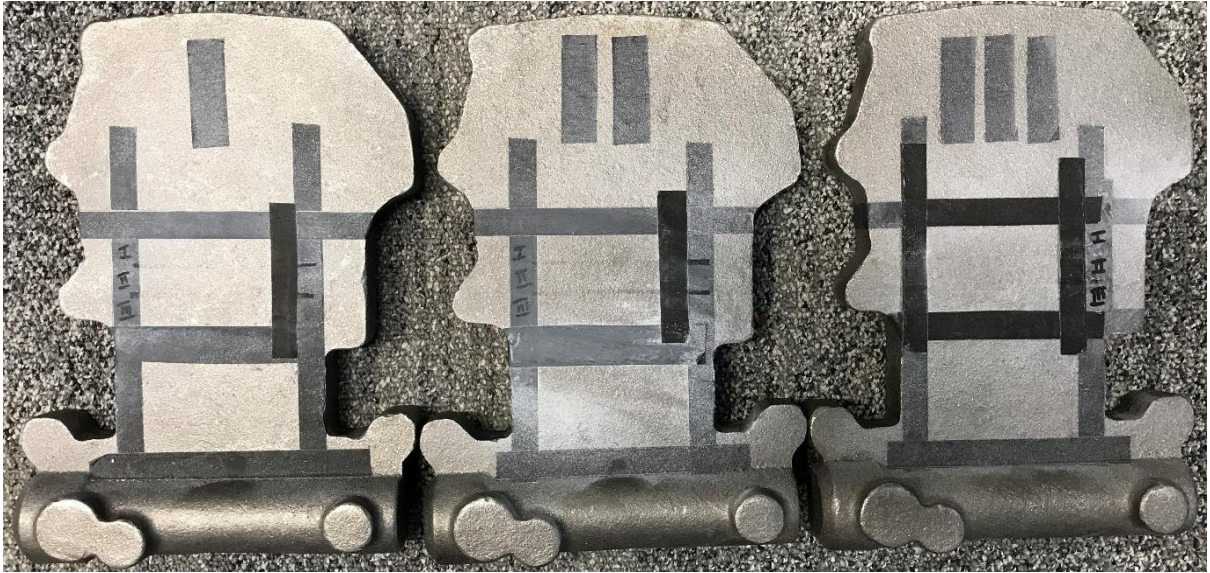


*Figure 33: Casting A: Sections within the hash marks of black masking tape represent areas of scanning on three identical surfaces*

It can be seen from Figure 34 that the box plots are small in size showcasing that the three castings have a smaller spread of data and the medians are at the same level. To verify these results, the scanned area from Casting A-1 is cut (Figure 35) and the sample is measured using the optical surface profiler as shown in the same figure.

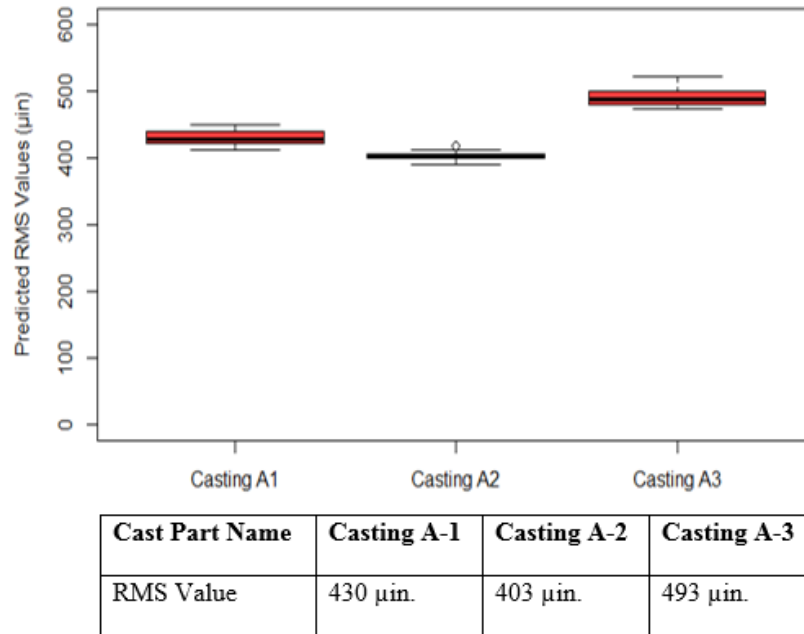


Figure 34: Box & Whisker plot showing the RMS comparison between the three identical patches of casting surface 'A' and the average RMS obtained on each of these surfaces.



Figure 35 : Cut samples from Casting A-1 and sample measurement on Zygo surface profiler and Mahr profilometer.

Measurement Precision of surface roughness on Casting A:

To determine the precision of the proposed measurement technique, laser scans are performed at 15 segments of the casting surface and the generated point clouds are run through the developed R program. The obtained average PCA values are then converted to the average Sq values using the established correlation curve built into the program. Similarly, roughness measurements made using the Mahr SD26 stylus profilometer and Zygo NewView 7100 laser interferometer are shown in Table 10 for comparisons. The recommended cut-off wavelengths as per ISO 4288 for non-periodic profiles are used for Mahr SD 26. The objective lens used for Zygo is 5X magnification with 150 $\mu$ m extended scan length. For the 15 readings, the *coefficient of variation* of the proposed laser scanning method is 2.52%, compared with 13.66% for the Zygo and 17.31% for the MahrSurf26. It is evident from the Table 9 that the proposed laser scanning method gives more consistent readings as opposed to the conventional stylus and interferometer method. This is due to the fact that the proposed method using laser scanners is based on ‘area sampling’ process which tends to give less variation in results compared to the line sampling used in MahrSD 26. Similarly, the variation in Zygo can be attributed to the small sample area that is scanned. Also, the relatively high cost of commercially available interferometer systems such as the Zygo has added to the obstacle. Moreover, these systems lack versatility since samples have to be machined to a small block for roughness measurements. There was not only an increase in time due to sample machining but also due to extended scan length times needed for cast surfaces as mentioned earlier. Hence, proposed method is not only repeatable, but also is time and cost efficient.

*Table 10: Repeatability of the roughness measurement on Casting sample –A1 by MahrSurf, Zygo and the proposed method*

<b>Reading No</b>	<b>MahrSurf26 (RMS, <math>\mu\text{in}</math>)</b>	<b>Zygo (RMS, <math>\mu\text{in}</math>)</b>	<b>Proposed method (RMS, <math>\mu\text{in}</math>)</b>
1	631	457	421
2	717	537	429
3	608	409	424
4	460	444	434
5	718	526	451
6	783	465	441
7	729	459	414
8	704	540	440
9	529	641	428
10	525	477	421
11	457	419	432
12	628	545	440
13	476	418	413
14	592	426	441
15	679	558	429
Average	616	488	430
Standard Deviation	106.55	66.68	10.86
<b>Coefficient of variation</b>	<b>17.31%</b>	<b>13.66%</b>	<b>2.52%</b>

## 2) Casting B:

For further validating the effectiveness of proposed method, castings with varying section thickness are chosen for the next set of laser scanning as shown in Figure 36:

However, it is discovered from the initial results that the surface roughness estimations are higher. A difference between the box plots (left) in Figure 37 for comparative groups was observed and further investigation was carried out to determine the cause. It was found that there are undercuts, surface bumps and huge surface waviness on some portions of the scanned area. The analysis of these segments after removing these surface irregularities from the point cloud provided consistent results and yielded a box plot as shown on the right.



*Figure 36: Sections of Casting B within the bottom part of black masking tape represent areas of scanning on three identical surfaces*

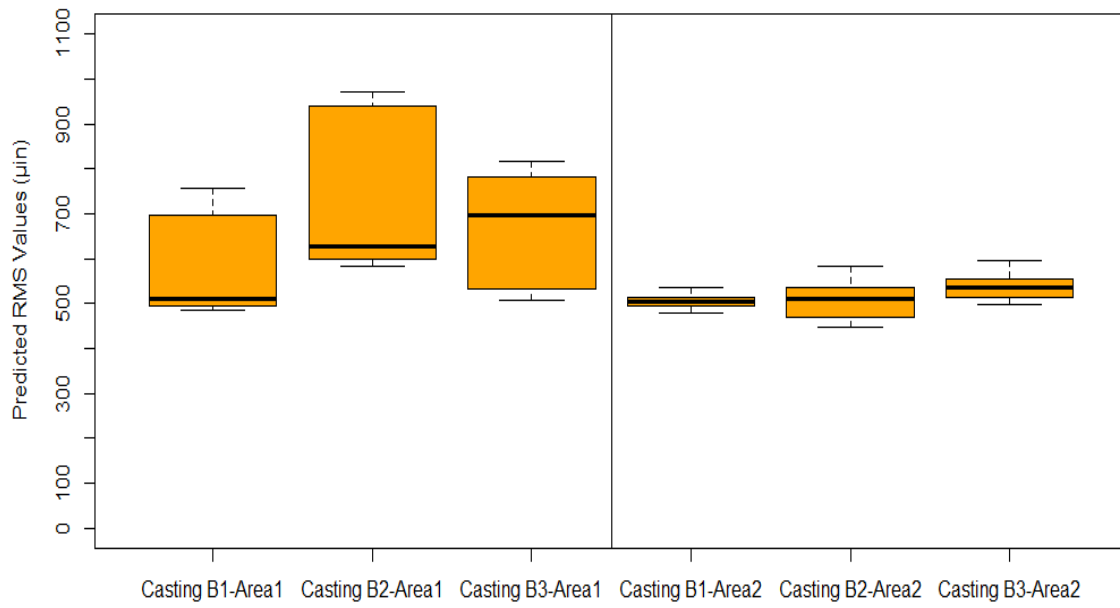


Figure 37: Box & Whisker plot showing the RMS comparison between the three identical patches of Casting B. For plot description, refer Figure 16.



Figure 38 : Cut samples from Casting B and sample measurement using Zygo surface profiler and Mahr profilometer

Measurement Precision of surface roughness on Casting B:

Similar to the calculations performed on Casting A, Casting B showed the following results as shown in Table 11. For the 15 readings, the coefficient of variation of the proposed laser scanning is 3.20% compared to 9.76% for Zygo and 12.95% for MahrSurf26.

*Table 11: Repeatability of the roughness measurement on Casting sample –B1 by MahrSurf, Zygo and the proposed method*

<b>Reading No</b>	<b>MahrSurf26 (RMS, <math>\mu\text{in}</math>)</b>	<b>Zygo (RMS, <math>\mu\text{in}</math>)</b>	<b>Proposed method (RMS, <math>\mu\text{in}</math>)</b>
1	806	587	479
2	809	517	484
3	810	538	503
4	599	497	536
5	868	444	492
6	746	536	512
7	809	573	528
8	784	607	494
9	815	598	514
10	627	497	509
11	899	520	497
12	821	437	514
13	627	501	516
14	871	524	487
15	627	485	500
Average	768	524	504
Standard Deviation	99.40	51.14	16.13
<b>Coefficient of variation</b>	<b>12.95%</b>	<b>9.76%</b>	<b>3.20%</b>

### 3) Casting C:

Finally, a larger casting which is a scaled-up version of Casting C (Figure 39) is scanned and the results showcased the same phenomenon as shown in Figure 31.



*Figure 39: Sections of three Casting C within black masking tape representing areas of scanning on three identical surfaces*

The trend of box plot in Figure 40 (left) is similar to the one in Figure 37 (left). This indicates that there is a source of error in surface roughness estimation on ‘Area 1’ of Casting C similar to Casting B. In other words, the results imply that a right surface roughness evaluation is not obtained on casting surfaces with non-continuous surface irregularities (protrusions and depressions). At the same time, the surface roughness measurements on ‘Area 2’ (after removal of irregularities) provided more consistent and reproducible results; thereby implying the reliability of the model for surfaces free from non-continuous surface irregularities. Hence, it would be wise to avoid laser scan of surfaces with visually noticeable defects such as undercuts, misrun, mechanical damages and burn-ons.

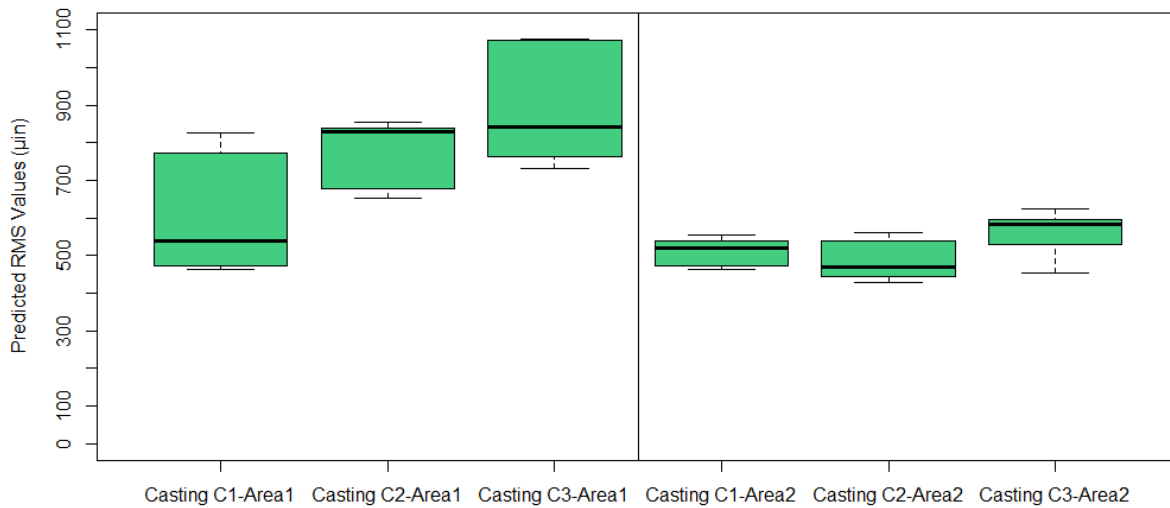


Figure 40: Box & Whisker plot showing the RMS comparison between the three identical patches of casting surface 'C' on different sectional areas of the casting. For plot description, refer Figure 16.



Figure 41: Cut sample from Casting C and sample measurement using Zygo surface profiler and Mahr profilometer.

#### Measurement Precision of surface roughness on Casting C:

Similar to the calculations performed on Casting A and B, Casting C showed the following results as shown in Table 12. For 15 readings, the co-efficient of variation of the proposed laser scanning is 6.88% compared to 11.90% for Zygo and 13.99% for MahrSurf.

*Table 12 : Repeatability of the roughness measurement on Casting sample –C1 by MahrSurf, Zygo and the proposed method*

<b>Reading No</b>	<b>MahrSurf26 (RMS, <math>\mu\text{in}</math>)</b>	<b>Zygo (RMS, <math>\mu\text{in}</math>)</b>	<b>Proposed method (RMS, <math>\mu\text{in}</math>)</b>
1	636	589	544
2	801	513	464
3	742	633	553
4	1065	580	521
5	759	653	476
6	852	568	531
7	677	585	533
8	783	589	471
9	901	559	538
10	892	655	479
11	737	498	464
12	717	522	548
13	873	428	495
14	851	612	468
15	673	462	540
Average	797	563	508
Standard Deviation	111.53	67.01	35
<b>Coefficient of variation</b>	<b>13.99%</b>	<b>11.90%</b>	<b>6.88%</b>

In addition to the huge variance observed on the costly metrological instruments shown above, it is also to be noted that they are not suited for heavy and large cast parts and often involve sampling of cast surfaces.

### Validating the Scanning Method Using a Portable 3D Scanner

For validating the proof of concept on a different 3D scanner, a hand-held Creaform HandyScan700 shown in Figure 42 with an accuracy of 30 microns and resolution of 100 microns is used.

To start with, a ‘C-9’ Comparator is scanned 11 times each on every specimen and



*Figure 42: HandyScan700 capturing point cloud of SCRATA plates*

the surface roughness values are estimated. Table 13 demonstrates similar pattern of interaction occurring between 20, 60 and 120  $\mu\text{in}$  roughness specimens of ‘C-9’ further validating the results obtained earlier using FARO laser line probe. The minimum threshold is found to be 200  $\mu\text{in}$ , but a minimal difference in PCA roughness value is observed. This can be attributed to the scanner’s accuracy of 30 microns and a resolution of 100 microns which is different from the FARO scanner.

Table 13: PCA values of 'C-9' comparator plate obtained at 95% CI using Creaform.

'C-9' Specimen Number	Flat	20	60	120	200
PCA Values (lower estimate, higher estimate) $\mu\text{in.}$	(956, 1046)	(1308, 1400)	(1353, 1390)	(1354, 1404)	(1450, 1502)

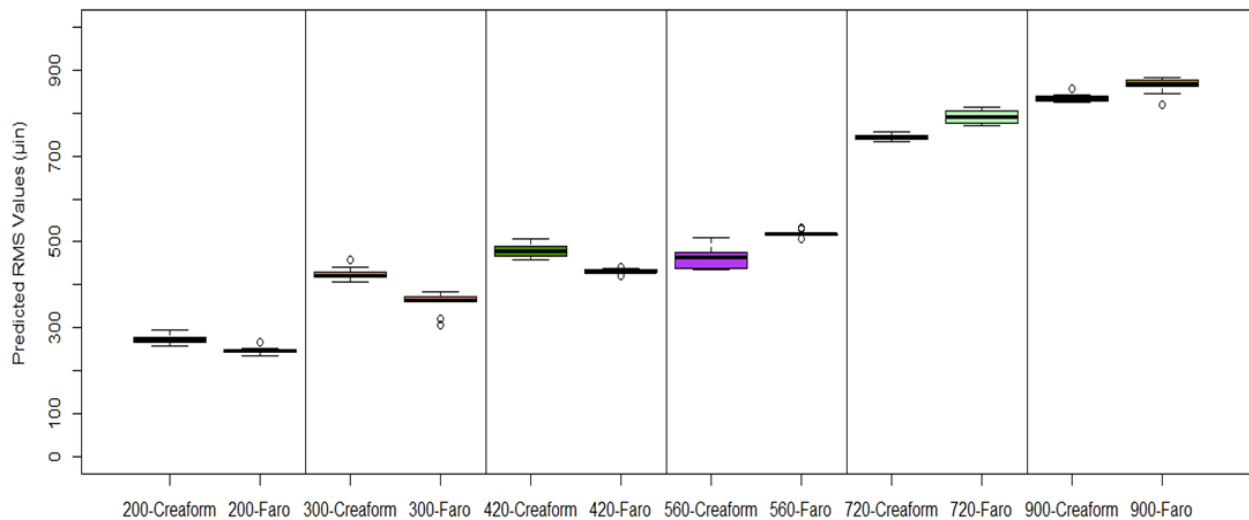


Figure 43: Box & Whisker plot showing the RMS comparison between Faro and Creaform for roughness specimens from 200-900.

As seen in Figure 43, it can be seen that there is an increasing trend in the average RMS values obtained using the Creaform Handy scanner and is comparatively similar to the scan results obtained using FaroArm Edge. This clearly demonstrates that the proposed method of non-contact 3D measurement gives consistent readings irrespective of the type of laser scanner used, provided the accuracy of the scanner is reasonably closer to the one used to build the proposed model.

Similarly, to validate the proposed approach on other known and unknown casting surfaces, roughness measurements are made using the hand-held scanner. The box plot of the results obtained using Creaform was compared to the previous results obtained by FaroArm Edge and is shown in Figure 44.

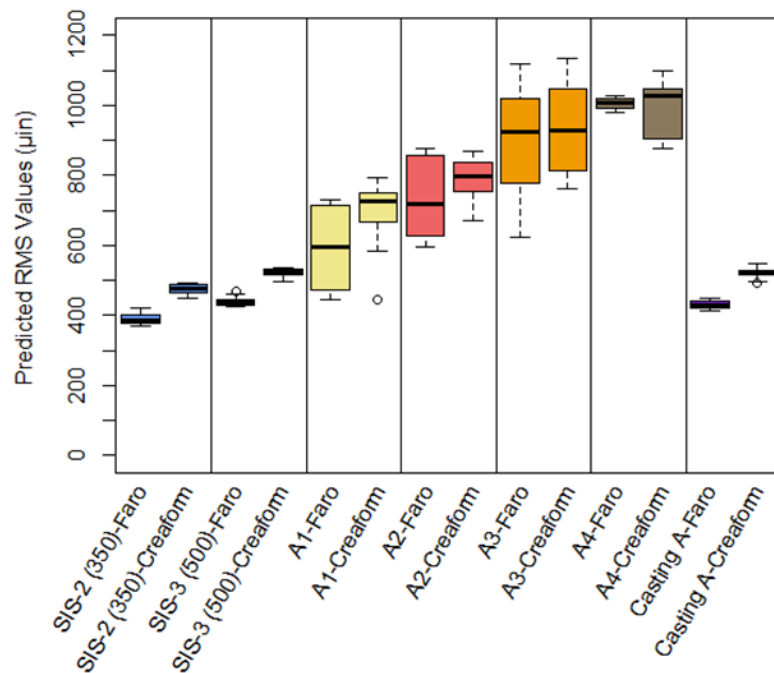


Figure 44: Roughness comparison between 3D scanners, Faro & Creaform on various comparators and casting surfaces.

From the above figure, it is observed that the median of the RMS values obtained from the two different scanners are close to each other. In some cases, the box plot comparisons show a difference in the median and spread of data and to further analyze this trend, 95% confidence interval is computed for SCRATA A-plates and tabulated as follows:

*Table 14: 95% confidence interval of SCRATA A-plates for Faro and Creaform*

	A1 (Faro)	A1 (Creaform)	A2 (Faro)	A2 (Creaform)	A3 (Faro)	A3 (Creaform)	A4 (Faro)	A4 (Creaform)
RMS Value(Lower estimate, Upper estimate) in $\mu\text{in}$	567,631	647,718	706,775	747,812	897,98 8	880,930	991,100 9	944, 1018

It can be inferred from Table 14 that the confidence intervals overlap between two different 3D laser scanners, namely the Faro and Creaform for A2, A3 and A4 surface texture plates. Nevertheless the confidence intervals for the lower roughness texture plate A1 did not yield a similar trend and this can be attributed to the difference in resolution between Faro and Creaform. However, it is safe to state that roughness measurements using different scanners yields similar trend in RMS values thereby validating the proof of concept.

#### **Zygo results on A1, A2, A3 and A4**

The non-contact laser interferometer “Zygo” used previously to validate the casting scan results is also used to validate the roughness results on A1-A4 as per ISO 4288. ‘A4’ cannot be measured by the Zygo even with the extended scan length due to machine limitations. The average roughness values calculated on the SCRATA plates at 3 different spots yielded results that were highly variable between different spots and yielded an average equivalent to the predicted RMS value as shown in Table 15.

Table 15: Average roughness measurements of SCRATA plates using Zygo surface profiler.

SCRATA Texture Levels	A1	A2	A3
<b>RMS Value (three sample points)</b>	498, 560, 749 ( $\mu\text{in.}$ )	724, 677, 737 ( $\mu\text{in.}$ )	852, 954, 869 ( $\mu\text{in.}$ )
<b>Average RMS Value</b>	602 $\mu\text{in.}$	712 $\mu\text{in.}$	892 $\mu\text{in.}$
<b>Standard Deviation</b>	130 $\mu\text{in}$	32 $\mu\text{in}$	55 $\mu\text{in}$

### Test on 3D printed metal casting surface

With emerging metal additive manufacturing (AM) technologies and surface texture research that is being on AM surfaces, two different SS316L (as fabricated) samples deposited by Direct Metal Laser Sintering are tested. 316L is an austenitic chromium-nickel stainless steel alloy with high strength and corrosion resistance. Since, they are reflective in nature, a developer spray was applied and scanning was performed. An average 'Sq' of 383  $\mu\text{in}$  (10  $\mu\text{m}$ ) with a standard deviation of 13.5  $\mu\text{in}$  (0.35  $\mu\text{m}$ ) is attained by using the proposed method.



Figure 45: SS316L sample as fabricated by DMLS process

The results obtained using the laser interferometer on the SS316L sample yielded an average RMS value of  $380 \mu\text{in}$  with a standard deviation of  $47.45 \mu\text{in}$  which was closer to the average RMS obtained by laser scanning.

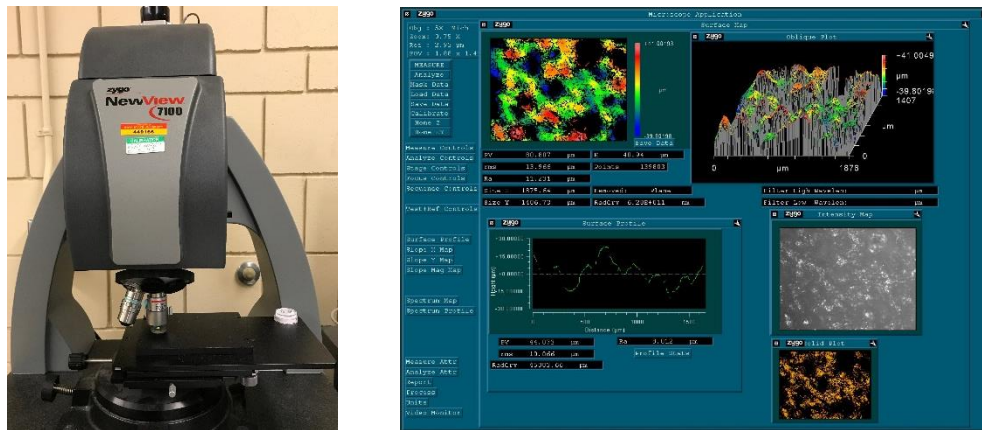


Figure 46: SS316L DMLS sample being measured by Zygo.

Hence, it is clear that the proposed PCA method for estimation of surface roughness is consistent for independent metal casting surfaces may it be from any kind of sand casting processes to additive manufactured, powder-bed laser-fused materials. Also, a study by Mower et al. (2016) uses the results obtained by an optical profilometer to understand the mechanical behavior of the additive materials. Consequently, with the proposed method which is comparatively repeatable, fast, versatile and accurate, these findings could be used to detect irregularities at an earlier stage which would help detect the formation of nucleation sites for cracks or any other discontinuity.

## CHAPTER 5

### CONCLUSIONS AND FUTURE WORK

From the study, the following conclusions are made:

- The validity of 3D laser scanning as a tool to measure the surface roughness of casting surfaces has been demonstrated by the use of PCA plane fitting on point cloud data using a developed R program
- The various factors such as shininess, limits of scanning system, depth of field, scanning direction and point density was studied and understood prior to running surface roughness computations.
- From the study, it was determined that the roughness values stated on the comparator plate were established after applying a filter cut-off wavelength. Since the proposed method does not remove longer wavelength components (waviness), the obtained PCA roughness values were different from the comparator roughness values.
- A correlation curve was then established using the known comparator specimens of ‘C-9’, followed by validation using an independent ‘ACI’ specimen. Following satisfactory results, the surface roughness of unknown surface texture plates of SCRATA is characterized in a quantitative manner.
- For casting surfaces, it is evident that the proposed technique of roughness estimation by area sampling (Sq) is not only consistent, but also has a lower coefficient of variation compared to the conventional methods of surface roughness measurements which rely on line sampling.

Without a quantitative method of surface characterization, the quality personnel are forced to such statements as “This castings *might* be either A2 or A3”. This subjectivity

involved in surface roughness approximations leads to ambiguity and confusion resulting in lost time, higher cost due to scrap, repair and dissatisfaction all along the production line. With the proposed method, we are able to accurately and consistently measure surface roughness on metal casting surfaces. Once integrated into the production line, this automated method to calculate the surface roughness from point cloud data will provide a fast output within few seconds and is the best road to good customer relations, reduced costs and ultimately improved profits. With the decreasing cost of 3D scanning technologies, 3D scanners would be the coming age of quantitatively examining a casting surface and evaluating its quality.

### Future Work

This method can be extended to estimate surface roughness on curved surfaces such as a cylindrical portion of the casting or a spherical casting surface by employing *Manifold Learning*, which is a non-linear version of Principal Component Analysis. After performing this operation, the best representation of the planar surface can be estimated which would serve as the nominal surface for surface roughness computations. However, this field is fairly new with many unsolved problems but would soon serve as a powerful tool to estimate surface roughness of curved surfaces and wavy casting surfaces. The approach described in this study can be used to validate any technology that can give the output in the form of a point cloud. In addition, the effect of abnormalities on surface roughness and methods to remove abnormalities can be explored

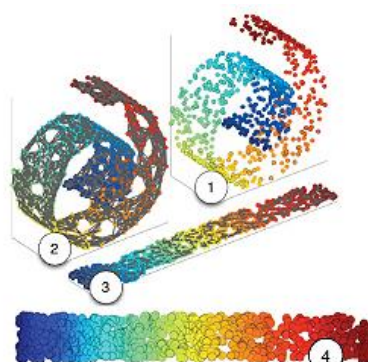


Figure 47: Unfolding of a Swiss roll by Manifold learning shown in stages from 1 to 4

## BIBLIOGRAPHY

1. AFS. "*Metalcasting Industry Information and Demographics.*" About AFS and Metalcasting. N.p., n.d. Web. 08 June 2017.  
<<http://www.afsinc.org/about/content.cfm?ItemNumber=13450>>.
2. AFS. "*Surface Finishes for Casting Processes.*" American Foundry Society, n.d. Web. 07 June 2017. <<http://www.afsinc.org/content.cfm?ItemNumber=6915>>.
3. Ambedkar, Rohit Vinay. Thesis submitted on "*Investigation of the Abilities of 3D Scanning Technology for Quality Inspection of Additively Manufactured Metal parts*" (2016)
4. ASME. *Surface Texture: Surface Roughness, Waviness and Lay*. New York: American Society of Mechanical Engineers, 2009. Print. ASME B46.1-2009.
5. ASTM International. *Standard Practice for Steel Castings, Surface Acceptance Standards, Visual Examination*. Tech. no. A802/A802M-95. West Conshohocken: ASTM Int&#39;l, 2006.
6. British Standards Institute, & European Committee for Standardization/Comit? European de Normalisation. (2012). "*Founding - Examination of Surface Condition*".
7. Curley, S. (2017). The advantages of investment casting's fine finish. *Aerospace Manufacturing*, 12(106), 1-42. doi:10.1520/b0618\_b0618m-08
8. Daricilar, G. "*Measurement Error of Visual Casting Surface Inspection*". M.S. Thesis, Iowa State University, 2005.
9. "FARO 3D Blog – "*Laser Scanning in a 3D Manufacturing World*" [Online]. Available: <http://blog.faro.com/2014/02/laser-scanning-in-a-3d-manufacturing-world/>. [Accessed: 04- July-2017]

10. FARO Edge and ScanArm ES Features , “*Benefits & Technical Specifications Edge and ScanArm*”. (2013.).
11. GAR Precision Reference Standard. (n.d.). Retrieved June 13, 2017, from <http://surfacefinishequipment.com/gar-standard.html>
12. GAR. (n.d.). “*Surface Roughness Scale for Surface Quality Control*” [Pamphlet]. Danbury, CT: GAR Electroforming Div Electroformers, Inc.
13. Gene H. Golub and Charles F. Van Loan. 1996. “*Matrix Computations (3rd Ed.)*”. Johns Hopkins University Press, Baltimore, MD, USA.
14. Golnabi, H., Asadpour, A., 2007. Design and application of industrial machine vision systems. *Robot. Comput. Integr. Manuf.* 23, 630–637.  
doi:<https://doi.org/10.1016/j.rcim.2007.02.005>
15. Groover, M. (2013).”*Fundamentals of modern manufacturing : Materials, processes, and systems*” / Mikell P. Groover. (5th ed.). Hoboken, NJ: John Wiley & Sons.
16. Hatamleh, O., Smith, J., Cohen, D., Bradley, R., 2009. “*Surface roughness and friction coefficient in peened friction stir welded 2195 aluminum alloy*”. *Appl. Surf. Sci.* 255, 7414–7426. doi:[10.1016/j.apsusc.2009.04.011](https://doi.org/10.1016/j.apsusc.2009.04.011)
17. Jolliffe, I. (1986). “*Principal Component Analysis*”. Springer Verlag.
18. Koçer, E., Horozoğlu, E., Asiltürk, I., 2015. “*Noncontact surface roughness measurement using a vision system*” 9445, 944525. doi:[10.1117/12.2180683](https://doi.org/10.1117/12.2180683)
19. Konstantoulakis, Nakajima, Woody, & Miller. (1998). Marginal fit and surface roughness of crowns made with an accelerated casting technique. *The Journal of Prosthetic Dentistry*, 80(3), 337-345.

20. Leach, R. (2014). *“Fundamental Principles of Engineering Nanometrology”* (2nd ed., Micro and Nano Technologies). Burlington: Elsevier Science.
21. Loftin G.E., & Schoefer E.A. (1970). *“Cast surface comparison standard”*. Google Patents. Retrieved from <https://www.google.com/patents/US3505861>
22. Luke, F., Huynh, V., North, W., 2000. *“Measurement of surface roughness by a machine vision system”*. J. Phys. E. 22, 977–980. doi:10.1088/0022-3735/22/12/001
23. Mower, T.M., Long, M.J., 2016. *“Mechanical behavior of additive manufactured, powder-bed laser-fused materials”*. Mater. Sci. Eng. A 651, 198–213.  
doi:10.1016/j.msea.2015.10.068
24. MSS. Quality Standard for Steel Castings for Valves, Flanges and Fittings and Other Piping Components (Visual Method). Tech. no. SP-55. New York: Manufacturers Standardization Society of the Valve and Fittings Industry, 1961.
25. Nwaogu, U., Poulsen, T., Gravesen, B., Tiedje, N., 2012. *“Using sol-gel component as additive to foundry coatings to improve casting quality”*. Int. J. Cast Met. Res. 25, 176–187. doi:10.1179/1743133611Y.0000000038
26. Nwaogu, Tiedje, & Hansen. (2013). *“A non-contact 3D method to characterize the surface roughness of castings”*. Journal of Materials Processing Tech., 213(1), 59-68.
27. Quinsat, & Tournier. (2011). *“In situ non-contact measurements of surface roughness”*. Precision Engineering, Precision Engineering.
28. Smith, B., 1993. *“Making war on defects Six-sigma design”*. IEEE Spectr. 30, 43–47.  
doi:10.1109/6.275174
29. Steel Founder’s Society of America. (1969). *“Standard for the Visual Inspection of Casting Surfaces”*

30. Swing, E., 1963 "*Methods of surface roughness measurement*". In: Transactions of the American Foundrymen's Society, Proceedings of the Sixty-Seventh Annual Meeting, vol. 71, 1964, IL, pp. 452-459
31. Tesfamariam, Ephrem. "*Thesis submitted on Comparing discontinuity surface roughness derived from 3D terrestrial laser scan data with traditional field-based methods*" (2007)
32. Wall, Michael E., Andreas Rechtsteiner, Luis M. Rocha. "*Singular value decomposition and principal component analysis*".
33. Watts, K., Peters, F., & Stone, R., "*Visual Inspection: Known factors that affect performance*". Proceedings of the 2010 Steel Founder's Society of America – Technical & Operating Conference.